Chapter 21
Biochemical fuel cells

Eugenii Katz, Andrew N. Shipway and Itamar Willner

Institute of Chemistry and The Farkas Center for Light-Induced Processes, The Hebrew University of Jerusalem, Jerusalem, 91904 Israel

1 INTRODUCTION

During the 20th century, energy consumption increased dramatically and an unbalanced energy management exists. While there is no sign that this growth in demand will abate (particularly amongst the developing nations), there is now an awareness of the transience of nonrenewable resources and the irreversible damage caused to the environment. In addition, there is a trend towards the miniaturization and portability of computing and communications devices. These energy-demanding applications require small, light power sources that are able to sustain operation over long periods of time, particularly in remote locations such as space and exploration. Furthermore, advances in the medical sciences are leading to an increasing number of implantable electrically operated devices (e.g., pacemakers). These items need power supplies that will operate for extremely long durations as maintenance would necessitate surgery. Ideally, implanted devices would take advantage of the natural fuel substances found in the body, and thus would continue to draw power for as long as the subject lives. Biofuel cells potentially offer solutions to all these problems, by taking nature's solutions to energy generation and tailoring them to our own needs. They take readily available substrates from renewable sources and convert them into benign by-products with the generation of electricity. Since they use concentrated sources of chemical energy, they can be small and light, and the fuel can even be taken from a living organism (e.g., glucose from the blood stream).

Biofuel cells use biocatalysts for the conversion of chemical energy to electrical energy.[1–8] As most organic substrates undergo combustion with the evolution of energy, the biocatalyzed oxidation of organic substances by oxygen or other oxidizers at two-electrode interfaces provides a means for the conversion of chemical to electrical energy. Abundant organic raw materials such as methanol, organic acids, or glucose can be used as substrates for the oxidation process, and molecular oxygen or H_2O_2 can act as the substrate being reduced. The extractable power of a fuel cell (P_{cell}) is the product of the cell voltage (V_{cell}) and the cell current (I_{cell}) (equation (1)). Although the ideal cell voltage is affected by the difference in the formal potentials of the oxidizer and fuel compounds ($E^{\circ\prime}_{ox} - E^{\circ\prime}_{fuel}$), irreversible losses in the voltage (η) as a result of kinetic limitations of the electron transfer processes at the electrode interfaces, ohmic resistances and concentration gradients, lead to decreased values (equation (2)).

$$P_{cell} = V_{cell} \times I_{cell} \tag{1}$$

$$V_{cell} = E^{\circ\prime}_{ox} - E^{\circ\prime}_{fuel} - \eta \tag{2}$$

Similarly, the cell current is controlled by the electrode sizes, the ion permeability and transport rates across the membrane separating the catholyte and anolyte compartments of the biofuel cell (specifically, the rate of electron transfer at the respective electrode surfaces). These different parameters collectively influence the biofuel cell power, and

Handbook of Fuel Cells – Fundamentals, Technology and Applications, Edited by Wolf Vielstich, Hubert A. Gasteiger, Arnold Lamm. Volume 1: *Fundamentals and Survey of Systems*.

for improved efficiencies, the V_{cell} and I_{cell} values should be optimized.

Biofuel cells can use biocatalysts, enzymes or even whole cell organisms in one of two ways.[1–8] Either (i) the biocatalysts can generate the fuel substrates for the cell by biocatalytic transformations or metabolic processes, or (ii) the biocatalysts may participate in the electron transfer chain between the fuel substrates and the electrode surfaces. Unfortunately, most redox enzymes do not take part in direct electron transfer with conductive supports, and therefore a variety of electron mediators (electron relays) are used for the electrical contacting of the biocatalyst and the electrode.[9] Recently, novel approaches have been developed for the functionalization of electrode surfaces with monolayers and multilayers consisting of redox enzymes, electrocatalysts and bioelectrocatalysts that stimulate electrochemical transformations at the electrode interfaces.[10] The assembly of electrically contacted bioactive monolayer electrodes could be advantageous for biofuel cell applications as the biocatalyst and electrode support are integrated. This article summarizes recent advances in the tailoring of conventional microbial-based biofuel cells and describes novel biofuel cell configurations based on biocatalytic interface structures integrated with the cathodes and anodes of biofuel cells.

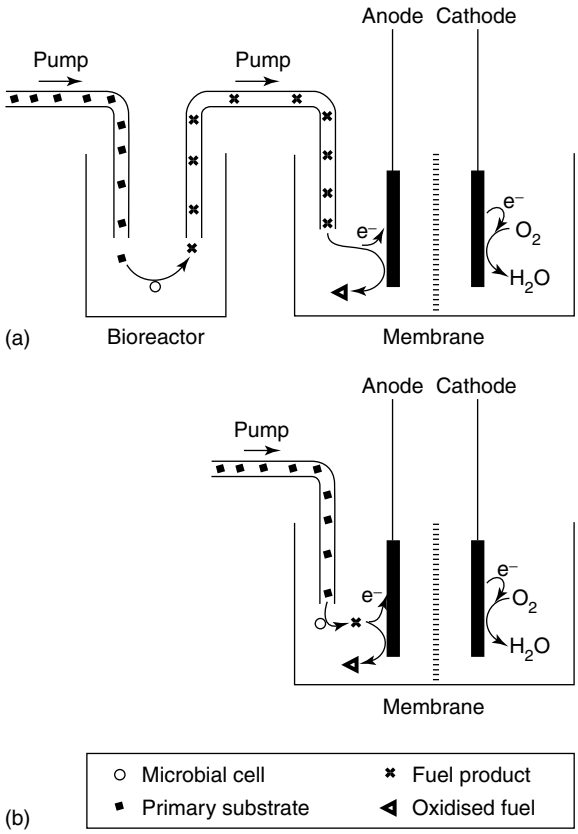

Figure 1. Schematic configuration of a microbial biofuel cell: (a) with a microbial bioreactor providing fuel separated from the anodic compartment of the electrochemical cell; (b) with a microbial bioreactor providing fuel directly in the anodic compartment of the electrochemical cell.

2 MICROBIAL-BASED BIOFUEL CELLS

The use of entire microorganisms as microreactors in fuel cells eliminates the need for the isolation of individual enzymes, and allows the active biomaterials to work under conditions close to their natural environment, thus at a high efficiency. Whole microorganisms can be difficult to handle, however, requiring particular conditions to remain alive, and their direct electrochemical contact with an electrode support is virtually impossible.

Microorganisms have the ability to produce electrochemically active substances that may be metabolic intermediaries or final products of anaerobic respiration. For the purpose of energy generation, these fuel substances can be produced in one place and transported to a biofuel cell to be used as a fuel. In this case the biocatalytic microbial reactor produces the biofuel and the biological part of the device is not directly integrated with the electrochemical part (Figure 1a). This scheme allows the electrochemical part to operate under conditions that are not compatible with the biological part of the device. The two parts can even be separated in time, operating completely individually. The most widely used fuel in this scheme is hydrogen gas, allowing well-developed and highly efficient H_2/O_2 fuel cells to be conjugated with a bioreactor.

According to another approach, the microbiological fermentation process proceeds directly in the anodic compartment of a fuel cell, supplying the anode with the in situ produced fermentation products (Figure 1b). In this case the operational conditions in the anodic compartment are dictated by the biological system, so they are significantly different from those in conventional fuel cells. At this point we have a real biofuel cell and not a simple combination of a bioreactor with a conventional fuel cell. This configuration is also often based on the biological production of hydrogen gas, but the electrochemical oxidation of H_2 is performed in the presence of the biological components under mild conditions. Other metabolic products (e.g., formate, H_2S) have also been used as fuels in this kind of system.

A third approach involves the application of artificial electron transfer relays that can shuttle electrons between the microbial biocatalytic system and the electrode. The

mediator molecules take electrons from the biological electron transport chain of the microorganisms and transport them to the anode of the biofuel cell. In this case, the biocatalytic process performed in the microorganisms becomes different from the natural one since the electron flow goes to the anode instead of to a natural electron acceptor. Since the natural electron acceptor is usually more efficient, it can compete with the desired scheme, so it is usually removed from the system. In most cases, the microbiological system operates under anaerobic conditions (when O_2 is removed from the system), allowing electron transport to the artificial electron relays and, finally, to the anode.

2.1 Microbial bioreactors producing H_2 for conventional fuel cells

Various bacteria and algae, for example *Escherichia coli*, *Enterobacter aerogenes*, *Clostridium butyricum*, *Clostridium acetobutylicum*, and *Clostridium perfringens* have been found to be active in hydrogen production under anaerobic conditions.[11–16] The most effective H_2 production is observed upon fermentation of glucose in the presence of *Clostridium butyricum* (strain IFO 3847, 35 μmol h^{-1} H_2 evolution by 1 g of the microorganism at 37 °C).[17] This conversion of carbohydrate to hydrogen is achieved by a multienzyme system. In bacteria the route is believed to involve glucose conversion to 2 mol of pyruvate and 2 mol of NADH by the Embden–Meyerhof pathway. The pyruvate is then oxidized through a pyruvate–ferredoxin oxidoreductase producing acetyl-CoA, CO_2, and reduced ferredoxin. NADH–ferredoxin oxidoreductase oxidizes NADH and reduces ferredoxin. The reduced ferredoxin is reoxidized by the hydrogenase to form hydrogen. As a result, 4 mol of hydrogen are produced from 1 mol of glucose under ideal conditions (equations (3)–(6)). However, only ca. 1 mol of H_2 per 1 mol of glucose was obtained under optimal conditions in a real system. Since the H_2 yield is only ca. 25% of the theoretical yield,[18] the improvement of hydrogen production by genetic engineering techniques and screening of new hydrogen-producing bacteria is possible for enhanced energy conversion. Glucose is an expensive substrate, and industrial wastewater containing nutritional substrates for H_2-producing bacteria have been successfully applied to produce hydrogen later used in a fuel cell.[17]

$$\text{Glucose} + 2\text{NAD}^+ \xrightarrow{\text{Multienzyme Embden–Meyerhof pathway}} 2\text{Pyruvate} + 2\text{NADH} \quad (3)$$

$$\text{Pyruvate} + \text{Ferredoxin}_{ox} \xrightarrow{\text{Pyruvate–ferredoxin oxidoreductase}} \text{Acetyl-CoA} + CO_2 + \text{Ferredoxin}_{red} \quad (4)$$

$$\text{NADH} + \text{Ferredoxin}_{ox} \xrightarrow{\text{NADH-ferredoxin oxidoreductase}} \text{NAD}^+ + \text{Ferredoxin}_{red} \quad (5)$$

$$\text{Ferredoxin}_{red} + 2H^+ \xrightarrow{\text{Hydrogenase}} \text{Ferredoxin}_{ox} + H_2 \quad (6)$$

The immobilization of hydrogen-producing bacteria, *Clostridium butyricum*, has great value because this stabilizes the relatively unstable hydrogenase system. In order to stabilize the biocatalytic performance, the bacteria were introduced into polymeric matrices, e.g., polyacrylamide,[17] agar gel,[19, 20] and filter paper.[18] The immobilized microbial cells continuously produced H_2 under anaerobic conditions for a period of weeks, whereas nonimmobilized bacteria cells were fully deactivated in less than 2 days.[19]

A H_2/O_2 fuel cell (Pt-black/nickel mesh anode and Pd-black/nickel mesh cathode separated by a nylon filter and operated at room temperature) was connected to a bioreactor (Jar-fermentor) producing H_2.[19, 20] The H_2 gas produced was collected and transported to the anodic compartment of the fuel cell, where the gas was used as a fuel (equation (7)). The current and voltage output were dependent on the rate of hydrogen production in the fermentor. For example, an open-circuit voltage (V_{oc}) of 0.95 V and short-circuit current density (i_{sc}) of 40 mA cm^{-2} were obtained at the H_2 flow of 40 ml min^{-1}. The biofuel cell operating at steady-state conditions for 7 days reveled a continuous current of between 500 and 550 mA.[20]

$$H_2 \longrightarrow 2H^+ + 2e^- (\text{to anode}) \quad (7)$$

2.2 Integrated microbial-based biofuel cells producing electrochemically active metabolites in the anodic compartment of biofuel cells

Microbial cells producing H_2 gas during fermentation have been immobilized directly in the anodic compartment of a H_2/O_2 fuel cell.[21, 22] A rolled Pt-electrode was introduced into a suspension of *Clostridium butyricum* microorganisms, then the suspension was polymerized with acrylamide to form a gel.[21] The fermentation was conducted directly at the electrode surface, supplying the anode with the H_2 fuel. In this case some additional by-products of the fermentation process (hydrogen, 0.60 mol; formic acid, 0.20 mol; acetic acid, 0.60 mol; lactic acid,

0.15 mol)[21] could also be utilized as additional fuel components. For example, pyruvate produced according to equation (3) can be alternatively oxidized to formate through a pyruvate–formate lyase (equation (8)).[17, 21] The metabolically produced formate is directly oxidized at the anode when the fermentation solution passes the anode compartment (equation (9)). The biofuel cell that included ca. 0.4 g of wet microbial cells (ca. 0.1 g of dry material) yielded upon optimal operating conditions the outputs $V_{cell} = 0.4\,V$ and $I_{cell} = 0.6\,mA$.[21]

$$\text{Pyruvate} \xrightarrow{\text{Pyruvate–formate lyase}} \text{Formate} \quad (8)$$

$$HCOO^- \longrightarrow CO_2 + H^+ + 2e^- (\text{to anode}) \quad (9)$$

It should be noted that in the case that a Pt-black electrode is used as an anode, oxidation of the original substrate utilized by the microorganisms in the fermentation process (e.g., glucose) can contribute to the anodic current. Thus, the H_2 provided by the microorganisms is the main, but not the only source of the anodic current.[23]

Other fuels have also been produced by microorganisms in the anodic compartments of biofuel cells. There are many microorganisms producing metabolically reduced sulfur-containing compounds (e.g., sulfides, S^{2-}, HS^-, sulfites, $SO_3{}^{2-}$). Sulfate-reducing bacteria (e.g., *Desulfovibrio desulfuricans*) form a specialized group of anaerobic microbes that use sulfate ($SO_4{}^{2-}$) as a terminal electron acceptor for respiration. These microorganisms yield S^{2-} while using a substrate (e.g., lactate) as a source of electrons (equation (10)). This microbiological oxidation of lactate with the formation of sulfide has been used to drive an anodic process in biofuel cells.[24, 25] The metabolically produced sulfide was oxidized directly at an electrode, providing an anodic reaction that produces sulfate or thiosulfate (equations (11) and (12)).

$$\text{Lactate} + SO_4{}^{2-} + 8H^+ \xrightarrow{\text{Bacteria}} S^{2-} + 4H_2O + \text{Pyruvate} \quad (10)$$

$$S^{2-} + 4H_2O \longrightarrow SO_4{}^{2-} + 8H^+ + 8e^- (\text{to anode}) \quad (11)$$

$$2S^{2-} + 3H_2O \longrightarrow S_2O_3{}^{2-} + 6H^+ + 8e^- (\text{to anode}) \quad (12)$$

The fermentation solution was composed of a microbe suspension (ca. 10^8 nonimmobilized cells per mL), with the nutritional substrates (mainly lactate) under anaerobic conditions. Accumulation of sulfides in the medium results in the inhibition of the metabolic bacteria process because of their interaction with iron containing proteins (e.g., cytochromes), causing the electron transport systems to be blocked. To prevent the toxic effect of H_2S, the anode should effectively oxidize it. However, many metallic electrodes are poisoned by sulfide because of its strong and irreversible adsorption. Thus, porous graphite electrodes were used (100 cm^2, impregnated with 10% (w/w) cobalt hydroxide, which in the presence of S^{2-} undergoes a transition into a catalytically highly active cobalt oxide/cobalt sulfide mixture).[24, 25] The biocatalytic anode was combined with an oxygen cathode (porous graphite electrode, 100 cm^2 geometrical area, activated with iron(II) phthalocyanine and vanadium(V) compounds) separated with a cation-exchange membrane in order to maintain anaerobic conditions in the anodic compartment. In a test study,[25] the electrical output of the biofuel element composed of three cells connected in series was $V_{oc} = 2.8\,V$ and $I_{sc} = 2.5–4.0\,A$ (i_{sc} = ca. 30 mA cm^{-2}). The element was loaded discontinuously for a period of 18 months, about 6 A being drawn from the cell for 40–60 min daily.

Microbiological fermentation under aerobic conditions utilizes O_2 as a terminal electron acceptor. It has been shown that aerobic fermentation of *Saccharomyces cerevisiae* or *Micrococcus cerificans* bacteria in the presence of glucose as the nutritional substrate in an anodic compartment of a biofuel cell results in an anodic current.[26–29] A biofuel cell in such a system works as an O_2-concentration cell utilizing the potential difference produced at the cathode and anode due to the oxygen consumption in the anodic compartment.

Table 1 summarizes the electrical output obtained in biofuel cells operating without electron transfer mediators and using the natural products of microbial fermentation (e.g., H_2, H_2S) as the current providing species.

2.3 Microbial-based biofuel cells operating in the presence of artificial electron relays

Reductive species generated by metabolic processes inside microbial cells are isolated from the external world by a microbial membrane. Thus, contact of the microbial cells with an electrode usually results in a very minute electron transfer across the membrane of the microbes.[30] In some specific cases, however, direct electron transfer from the microbial cells to an anode surface is still possible. The metal-reducing bacterium *Shewanella putrefaciens* MR-1 has been reported to have cytochromes in its outer membrane.[31] These electron carriers (i.e., cytochromes) are able to generate anodic current in the absence of terminal electron acceptors (under anaerobic conditions).[32, 33] However, this is a rather exceptional example.

Table 1. Examples of microbial-based biofuel cells utilizing fermentation products for their oxidation at anodes.[a]

Microorganism	Nutritional substrate	Fermentation product	Biofuel cell voltage	Biofuel cell current or current density	Anode[c]	Ref.
Clostridium butyricum	Waste water	H_2	0.62 V (at 1 Ω)	0.8 A (at 2.2 V)	Pt-blackened Ni, 165 cm^2 (5 anodes in series)	[19]
Clostridium butyricum	Molasses	H_2	0.66 V (at 1 Ω)	40 mA cm^{-2} (at 1 Ω)[b]	Pt-blackened Ni, 85 cm^2	[20]
Clostridium butyricum	Lactate	H_2	0.6 V (oc)[d]	120 μA cm^{-2} (sc)[e]	Pt-black, 50 cm^2	[21]
Enterobacter aerogenes	Glucose	H_2	1.04 V (oc)	60 μA cm^{-2} (sc)	Pt-blackened stainless steel, 25 cm^2	[22]
Desulfovibrio desulfuricans	Dextrose	H_2S	2.8 V (oc)	1 A	Graphite, $Co(OH)_2$ impregnated (3 anodes in series)	[25]

[a]In most studies the biofuel anode was conjugated with an O_2-cathode.
[b]The value calculated from other data using Ohm's law.
[c]The anode surface area is given as a geometrical area.
[d]Open-circuit measurements.
[e]Short-circuit measurements.

Low molecular weight redox species may assist the shuttling of electrons between the intracellular bacterial space and an electrode. However, there are many important requirements that such a mediator should satisfy in order to provide an efficient electron transport from the bacterial metabolites to the anode: (a) The oxidized state of the mediator should easily penetrate the bacterial membrane to reach the reductive species inside the bacterium. (b) The redox potential of the mediator should fit the potential of the reductive metabolite (the mediator potential should be positive enough to provide fast electron transfer from the metabolite, but it should not be so positive as to prevent significant loss of potential). (c) Neither oxidation state of the mediator should interfere with other metabolic processes (should not inhibit them or be decomposed by them). (d) The reduced state of the mediator should easily escape from the cell through the bacterial membrane. (e) Both oxidation states of the mediator should be chemically stable in the electrolyte solution, they should be well soluble, and they should not adsorb on the bacterial cells or electrode surface. (f) The electrochemical kinetics of the oxidation process of the mediator-reduced state at the electrode should be fast (electrochemically reversible).[8]

Many different organic and organometallic compounds have been tested in combination with bacteria to test the efficiency of mediated electron transport from the internal bacterial metabolites to the anode of a biofuel cell. Thionine has been used extensively as a mediator of electron transport from *Proteus vulgaris*[34–38] and from *Escherichia coli*.[38, 39] Other organic dyes that have been tested include benzylviologen, 2,6-dichlorophenolindophenol, 2-hydroxy-1,4-naphthoquinone, phenazines (phenazine ethosulfate, safranine), phenothiazines (alizarine brilliant blue, *N*, *N*-dimethyl-disulfonated thionine, methylene blue, phenothiazine, toluidine blue) and phenoxazines (brilliant cresyl blue, gallocyanine, resorufin).[36, 38–44] These organic dyes were tested with *Alcaligenes eutrophus*, *Anacystis nidulans*, *Azotobacter chroococcum*, *Bacillus subtilis*, *Clostridium butyricum*, *Escherichia coli*, *Proteus vulgaris*, *Pseudomonas aeruginosa*, *Pseudomonas putida* and *Staphylococcus aureus* bacteria, usually using glucose and succinate as substrates. Among the dyes tested, phenoxazine, phenothiazine, phenazine, indophenol, bipyridilium derivatives, thionine and 2-hydroxy-1,4-naphthoquinone were found to be very efficient in maintaining relatively high cell voltage output when current was drawn from the biofuel cell.[36] Some other dyes did not function as effective mediators because they are not rapidly reduced by microorganisms, or they lacked sufficiently negative potentials. Ferric chelate complexes (e.g., Fe(III)EDTA) were successfully used with *Lactobacillus plantarum*, *Streptococcus lactis* and *Erwinia dissolvens*, oxidizing glucose.[45]

Since thionine has frequently been used as a mediator in microbial biofuel-based cells, mono and disulfonated derivatives of thionine have been applied to determine the effect of hydrophilic substituents on the mediation of electron transfer from *Escherichia coli* to an anode.[46] Changing from thionine to 2-sulfonated thionine and 2,6-disulfonated thionine results in an increase in the efficiency of the mediated electron transport. This increase is reflected by changes in the biofuel cell current under a 560 Ω load – 0.35, 0.45 and 0.6 mA for thionine, monosulfo- and

Table 2. Redox potentials of electron relays used in microbial-based biofuel cells and the kinetics of their reduction by microbial cells.[a]

Redox relay	Structural formula	Redox potential (V vs. NHE)[b]	Rate of reduction (μmol (g dry wt)$^{-1}$ s^{-1})[c]
2,6-Dichlorophenol-indophenol	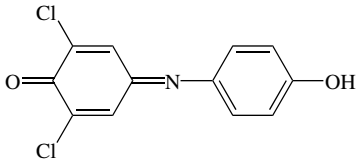	0.217	0.41
Phenazine ethosulphate	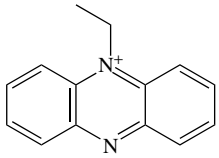	0.065	8.57
Safranine-O	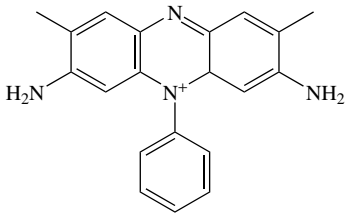	−0.289	0.07
N,*N*-Dimethyl-disulphonated thionine	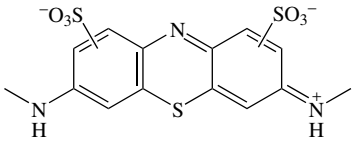	+0.220	0.33
New Methylene Blue	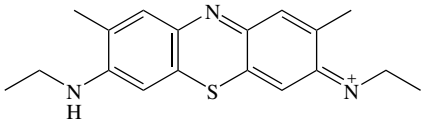	−0.021	0.20
Phenothiazinone	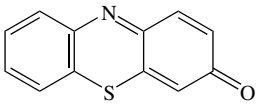	+0.130	1.43
Thionine	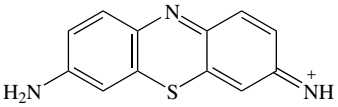	+0.064	7.10
Toluidine Blue-O	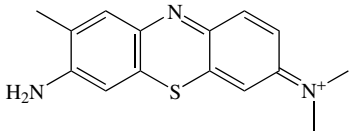	+0.034	1.47
Gallocyanine	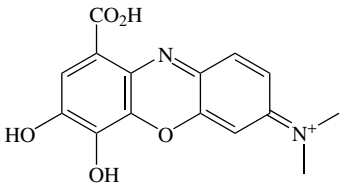	+0.021	0.53

Table 2. (*continued*)

Redox relay	Structural formula	Redox potential (V vs. NHE)[b]	Rate of reduction (μmol (g dry wt)$^{-1}$ s^{-1})[c]
Resorufin	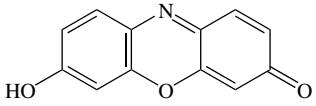	−0.051	0.61

[a]The data are taken from Ref. [38].
[b]$E^{\circ\prime}$ at pH 7.0. NHE, normal hydrogen electrode.
[c]The dye reduction by *Proteus vulgaris* at 30 °C, with 50 μM dye and 0.10–0.15 mg (dry wt) mL^{-1} of microbial cells. The oxidizable substrate is glucose.

disulfo-derivatives, respectively. The low efficiencies of the biofuel cells operating with thionine and 2-sulfonated thionine were attributed to interference to electron transfer by adsorption of the mediator on the microbial membrane. Table 2 summarizes the structures and redox potentials of electron transfer mediators as well as the rate constants of their reduction by microorganisms. It should be noted that the overall efficiency of the electron transfer mediators also depends on many other parameters, and in particular on the electrochemical rate constant of mediator re-oxidation, which depends on the electrode material.

Since an electron transfer mediator needs to meet many requirements, some of which are mutually exclusive, it is not possible to reach perfect conditions for electron transport from a bacterial cell to an electrode. A mixture of two mediators can be useful in optimizing the efficiency. A solution containing thionine and Fe(III)EDTA was applied to mediate electron transport from *Escherichia coli*, oxidizing glucose as a primary substrate to an anode.[47] Although both mediators can be reduced by the *Escherichia coli*, thionine is reduced over 100 times faster than Fe(III)EDTA. The electrochemical oxidation of the reduced thionine is much slower than oxidation of Fe(II)EDTA, however. Therefore, electrons obtained from the oxidation of glucose in the presence of *Escherichia coli* are transferred mainly to thionine under the operational conditions of the cell. The reduced thionine is rapidly re-oxidized by Fe(III)EDTA, the rate of which has been shown to be very fast, $k_{et} = 4.8 \times 10^4\,M^{-1}\,s^{-1}$. Finally, the reduced chelate complex, Fe(II)EDTA, transfers electrons to the anode by the electrode reaction of a Fe(III)EDTA/Fe(II)EDTA couple with a sufficiently large rate constant, $k_{el} = 1.5 \times 10^{-2}\,cm\,s^{-1}$. One more example of the enhanced electron transport in the presence of a mixture of mediators has been shown for *Bacillus* strains oxidizing glucose as a primary substrate. The biofuel cell was operating in the presence of methylviologen (MV^{2+}) and 2-hydroxy-1,4-naphthoquinone or Fe(III)EDTA.[16] Methylviologen can efficiently accept electrons from the bacterial cells, but its reduced state ($MV^{\bullet+}$) is highly toxic for the bacteria and immediately inhibits the fermentation process. In the presence of a secondary mediator that has a more positive potential, $MV^{\bullet+}$ is efficiently re-oxidized to MV^{2+}. The reduced secondary mediator (quinone or Fe(II)EDTA) then transports the electrons to the anode.

Engineering of the electrochemical cell provides a means of enhancing the electrical contact between a biocatalytic system and an anode and to improve the cell output. The interfacial contact has been increased using a three-dimensional packed bed anode.[48] The anode compartment was filled with graphite particles mixed with *Escherichia coli* bacteria, glucose as a primary electron source, and 2-hydroxy-1,4-naphthoquinone as a diffusional mediator. The bed electrode provided an active surface area 27.4-fold larger than the cross-sectional area of the anodic compartment, thus, the anodic current extracted was increased by an order of magnitude over a plate electrode.

In order to organize an integrated biocatalytic assembly in the anode compartment of a biofuel cell, the microbial cells and the electron transfer mediator should be co-immobilized at the anode surface. This goal is, however, very difficult to achieve since the electron transfer mediator needs to have some freedom to reach the intracellular bacterial space to interact with the metabolic species. In fact, the co-immobilization of bacterial cells with electron transfer mediators is much more difficult than the co-immobilization of redox enzymes with their respective mediators because in the case of microbial cells, the active species are isolated within a cellular membrane. This problem has been addressed using several methods. Neutral red **(1)**, an organic dye known to be an active diffusional mediator for electron transport from *Escherichia coli*,[40] has been covalently linked to a graphite electrode by making an amide bond between a carboxylic group on the electrode surface and an amino group of the dye[49] (Figure 2a). The mediator-modified electrode was used as an anode in the presence of *Escherichia coli*, and the surface-bound dye provided electron transfer

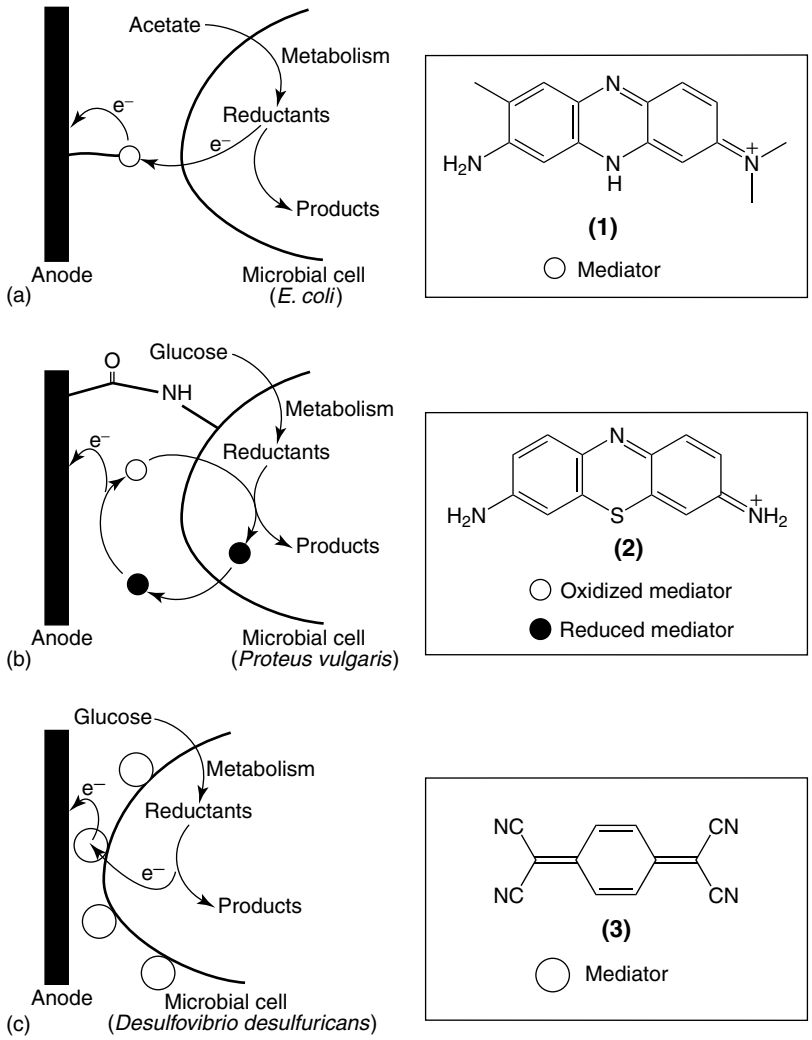

Figure 2. Electrical wiring of microbial cells to the anode of the electrochemical cell using electron transfer mediators: (a) a diffusional mediator shuttling between the microbial suspension and the anode surface; (b) a diffusional mediator shuttling between the anode and microbial cells covalently linked to the electrode; (c) a mediator adsorbed on the microbial cells providing the electron transport from the cells to the anode.

from the microbial cells to the conductive support under anaerobic conditions. In this case, only those bacteria that reached the modified electrode surface were electrically contacted. *Proteus vulgaris* microbial cells have been covalently bound to an oxidized carbon electrode surface by making amide bonds between carboxylic groups on the electrode surface and amino groups of the microbial membrane[50] (Figure 2b). An electrode modified with the attached microorganisms was applied as an anode in a biofuel cell in the presence of glucose as a primary reductive substrate and thionine (**2**) as a diffusional electron mediator. The microbe-modified anode showed an enhanced current output and better stability in comparison with a system composed of the same components but with nonimmobilized cells. *Desulfovibrio desulfuricans* microbial cells were covered by a polymeric derivative of viologen or modified by tetracyanoquinodimethane-2,2-(cyclohexa-2,5-diene-1,4-diylidene)bis(propane-1,3-dinitrile) (TCNQ) (**3**) adsorbed on the surface of the microbial cell[51] (Figure 2c). The microbial cells functionalized with the electron transfer mediators were applied in a biofuel cell providing a current to an anode in the absence of a diffusional mediator.

Microbial cells have also been grown in the presence of various nutritional substrates. For example, *Proteus vulgaris* bacteria were grown using glucose, galactose, maltose, trehalose and sucrose as primary electron donors and used in a biofuel cell with thionine as a diffusional electron transfer mediator.[34, 35, 37] Hydrocarbons such as *n*-hexadecane (using *Micrococcus cerificans*)[52] and methane (using *Pseudomonas methanica*)[53] have also been used as fuels to maintain anodic current in the anodic compartment of a biofuel cell. It has been shown that biofuel cell

Table 3. Examples of microbial-based biofuel cells utilizing electron relays for coupling of the intracellular electron transfer processes with electrochemical reactions at anodes.[a]

Microorganism	Nutritional substrate	Mediator	Biofuel cell voltage	Current or current density	Anode[c]	Ref.
Pseudomonas methanica	CH_4	1-Naphthol-2-sulfonate indo-2,6-dichlorophenol	5–6 V (oc)[d]	2.8 μA cm^{-2} (at 0.35 V)	Pt-black, 12.6 cm^2	[54]
Escherichia coli	Glucose	Methylene blue (**15**)	0.625 V (oc)	–	Pt, 390 cm^2	[42]
Proteus vulgaris, *Bacillus subtilis*, *Escherichia coli*	Glucose	Thionine	0.64 V (oc)	0.8 mA (at 560 Ω)	Reticulated vitreous carbon, 800 cm^2	[36]
Proteus vulgaris	Glucose	Thionine	350 mV (at 100 Ω)[b]	3.5 mA (at 100 Ω)	Reticulated vitreous carbon, 800 cm^2	[35]
Proteus vulgaris	Sucrose	Thionine	350 mV (at 100 Ω)[b]	3.5 mA (at 100 Ω)	Carbon	[34]
Escherichia coli	Glucose	Thionine	390 mV (at 560 Ω)[b]	0.7 mA (at 560 Ω)	_	[46]
Lactobacillus plantarum, *Streptococcus lactis*	Glucose	Fe(III)EDTA	0.2 V (oc)	90 μA (at 560 Ω)[b]	_	[45]
Erwinia dissolvens	Glucose	Fe(III)EDTA	0.5 V(oc)	0.7 mA (at 560 Ω)[b]	_	[45]
Proteus vulgaris	Glucose	2-Hydroxy-1,4-naphthoquinone	0.75 V (oc)	0.45 mA (at 1 kΩ)	Graphite felt, 1 g (0.47 m^2 g^{-1})	[51]
Escherichia coli	Acetate	Neutral Red (**1**)	0.25 V (oc)	1.4 μA cm^{-2} (sc)[e]	Graphite, 100 cm^2	
Escherichia coli	Glucose	Neutral Red (**1**)	0.85 V (oc)	17.7 mA (sc)	Graphite felt, 12 g (0.47 $m^2 g^{-1}$)	[40]
Escherichia coli	Glucose	2-Hydroxy-1,4-naphthoquinone	0.53 V (at 10 kΩ)	0.18 mA cm^{-2} (sc)	Glassy carbon, 12.5 cm^2	[49]

[a]In most studies the biofuel anode was conjugated with an O_2 cathode.
[b]The value calculated from other data using Ohm's law.
[c]The anode surface is given as a geometrical surface.
[d]Open-circuit measurements.
[e]Short-circuit measurements.

performance depends heavily on the primary substrate used in the fermentation process. The metabolic process in the bacteria is very complex, involves many enzymes, and may proceed by many different routes. It has been shown that a mixture of nutritional substrates can result even in higher extractable current than any single component alone.[54] It is possible to achieve maximum fuel cell efficiency just by changing the carbon source and thus inducing various metabolic states inside the microorganism. Table 3 summarizes the electrical output of microbial biofuel cells operating with different electron transfer mediators as species providing anodic current, and using different nutrients.

3 ENZYMATIC BIOFUEL CELLS

Microbial biofuel cells require the continuous fermentation of whole living cells performing numerous physiological processes, and thus dictate stringent working conditions. In order to overcome this constraint, the redox enzymes responsible for desired processes may be separated and purified from living organisms and applied as biocatalysts in biofuel cells rather than using the whole microbial cells.[1–6] That is, rather than utilizing the entire microbial cell apparatus for the generation of electrical energy, the specific enzyme(s) that oxidize(s) the target fuel-substrate may be electrically contacted with the electrode of the biofuel cell element. Enzymes are still sensitive and expensive chemicals, and thus special ways for their stabilization and utilization must be established.

Upon utilizing enzymes as catalytically active ingredients in biofuel, one may apply oxidative biocatalysts in the anodic compartments for the oxidation of the fuel-substrate and transfer of electrons to the anode, whereas reductive biocatalysts may participate in the reduction of the oxidizer in the cathodic compartment of the biofuel cell. Redox enzymes lack, however, direct electrical communication with electrodes due to the insulation of the redox center from the conductive support by the protein matrices.

Several methods have been applied to electrically contact redox enzymes and electrode supports.[9, 10, 55]

In the following sections, the engineering of biocatalytic electrodes for the oxidation of potential fuel substrates (biocatalytic anodes) and for the reduction of oxidizers (biocatalytic cathodes) is described. These electrodes are then integrated into biofuel cell elements and the output efficiencies of the bioelectronic devices are addressed.

3.1 Anodes for biofuel cells based on enzyme-catalyzed oxidative reactions

The electrochemical oxidation of fuels can be biocatalyzed by enzymes communicating electrically with electrodes. Different classes of oxidative enzymes (e.g., oxidases, dehydrogenases) require the application of different molecular tools to establish this electrical communication.[9, 10] Electron transfer mediators shuttling electrons between the enzyme active centers and electrodes are usually needed for the efficient electrical communication of flavin adenine dinucleotide FAD-containing oxidases (e.g., glucose oxidase (GOx)). $NAD(P)^+$-dependent dehydrogenases (e.g., lactate dehydrogenase) require $NAD(P)^+$-co-factor and an electrode catalytically active for the oxidation of NAD(P)H and regeneration of $NAD(P)^+$ to establish an electrical contact with the electrode.

3.1.1 Anodes based on the bioelectrocatalyzed oxidation of NAD(P)H

The nicotinamide redox co-factors (NAD^+ and $NADP^+$) play important roles in biological electron transport, acting as carriers of electrons and activating the biocatalytic functions of dehydrogenases, the vast majority of redox enzymes. The application of $NAD(P)^+$-dependent enzymes (e.g., lactate dehydrogenase, EC 1.1.1.27; alcohol dehydrogenase, EC 1.1.1.71; glucose dehydrogenase, EC 1.1.1.118) in biofuel cells allows the use of many organic materials such as lactate, glucose and alcohols as fuels. The biocatalytic oxidation of these substrates requires the efficient electrochemical regeneration of $NAD(P)^+$-co-factors in the anodic compartment of the cells. The biocatalytically produced NAD(P)H co-factors participating in the anodic process transports electrons from the enzymes to the anode, and the subsequent electrochemical oxidation of the reduced co-factors regenerates the biocatalytic functions of the system.

In aqueous solution at pH 7.0, the thermodynamic redox potential ($E^{\circ\prime}$) for $NAD(P)^+$/NAD(P)H is ca. -0.56 V (vs. the saturated calomel electrode (SCE)) – sufficiently negative for anode operation. Electrochemistry of NAD(P)H has been studied extensively, and it has been demonstrated that the electrochemical oxidation process is highly irreversible and proceeds with large overpotentials (η) (ca. 0.4, 0.7 and 1 V vs. SCE at carbon, Pt and Au electrodes, respectively).[9, 56] Strong adsorption of NAD(P)H and $NAD(P)^+$ (e.g., on Pt, Au, glassy carbon and pyrolytic graphite) generally poisons the electrode surface and inhibits the oxidation process. Furthermore, $NAD(P)^+$ acts as an inhibitor for the direct oxidation of NAD(P)H, and adsorbed NAD(P)H can be oxidized to undesired products that lead to the degradation of the co-factor (e.g., to NAD^+-dimers). Thus, the noncatalyzed electrochemical oxidation of NAD(P)H is not appropriate for use in workable biofuel cells. For the efficient electrooxidation of NAD(P)H, mediated electrocatalysis is necessary.[9, 56] Several immobilization techniques have been applied for the preparation of mediator-modified electrodes: The mediator molecules can be adsorbed directly onto electrodes, incorporated into polymer layers, or covalently linked to functional groups on electrode surfaces.[56]

A biofuel cell based on the electrocatalytic regeneration of NAD^+ at a modified anode has been developed.[57] Glucose dehydrogenase (EC 1.1.1.47) was immobilized in a porous glass located in the anode compartment of the biofuel cell. The enzyme oxidized the substrate (glucose) and produced the reduced state of the co-factor (NADH). The reduced co-factor reached the anode surface diffusionally (Meldola Blue was adsorbed at the graphite electrode, ca. 1×10^{-9} mol cm^{-2}), where it was oxidized to NAD^+. The biocatalytic anode was coupled to a Pt-cathode that reduced water to hydrogen and the biofuel cell provided $V_{oc} = 300$ mV and $i_{sc} = 220\,\mu$A cm^{-2} over a period of several hours.

The covalent coupling of redox mediators to self-assembled monolayers on Au-electrode surfaces has an important advantage for the preparation of multi-component organized systems.[58] Pyrroloquinoline quinone (PQQ, (**4**)) can be covalently attached to amino groups of a cystamine monolayer assembled on a Au surface (Figure 3a). The resulting electrode demonstrates good electrocatalytic activity for NAD(P)H oxidation, particularly in the presence of Ca^{2+}-cations as promoters (Figure 3b).[59] A quasi-reversible redox wave at the formal potential, $E^{\circ\prime} = -0.155$ V (vs. SCE at pH 8.0) is observed, corresponding to the two-electron redox process of the quinone units (Figure 3b, curve 1). Coulometric analysis of the quinone redox wave indicates that the PQQ surface coverage on the electrode is 1.2×10^{-10} mol cm^{-2}, a value that is typical for monolayer coverage. The electron transfer rate constant was found to be $k_{et} = 8$ s^{-1}. Figure 3b, curve 2, shows a cyclic voltammogram of a PQQ-functionalized electrode upon the addition of NADH (10 mM) in the presence of Ca^{2+}-ions. An electrocatalytic anodic current is observed in the presence

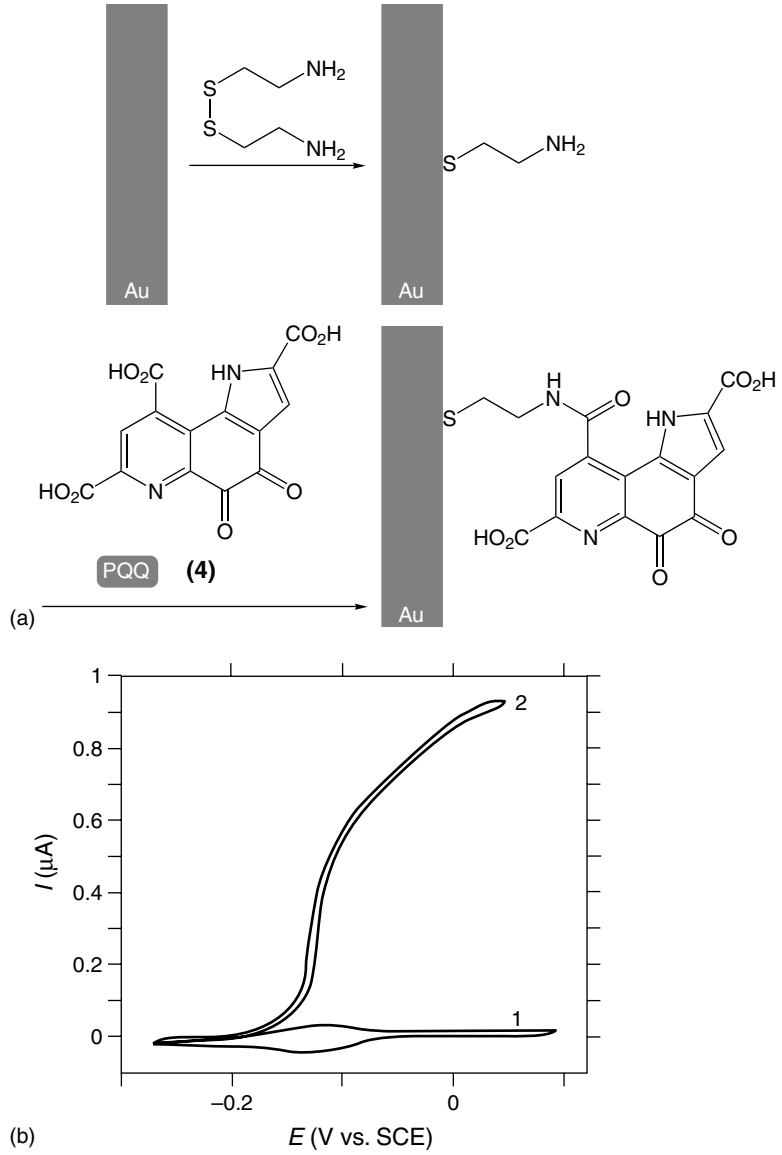

Figure 3. (a) Assembly of the PQQ-modified Au-electrode. (b) Cyclic voltammograms of a Au-PQQ electrode (geometrical area 0.2 cm^2, roughness factor ca. 1.5) in the presence of: (1) 0.1 M Tris–buffer, pH 8.0; (2) 10 mM NADH and 20 mM Ca^{2+}. Recorded at a scan rate of 1 mV s^{-1}.

of NADH, implying the effective electrocatalyzed oxidation of the co-factor, equations (13) and (14).

$$NADH + PQQ + H^+ \longrightarrow NAD^+ + PQQH_2 \qquad (13)$$

$$PQQH_2 \longrightarrow PQQ + 2H^+ + 2e^-(\text{to anode}) \qquad (14)$$

$NAD(P)^+$-dependent enzymes electrically contacted with electrode surfaces can provide efficient bioelectrocatalysis for NAD(P)H oxidation. For example, diaphorase (EC 1.6.4.3) was applied to oxidize NADH using a variety of quinone compounds, several kinds of flavins and viologens as mediators.[60] The bimolecular reaction rate constants between the enzyme and mediators whose redox potentials are more positive than −0.28 V (vs. SCE) at pH 8.5 can be as high as $10^8\ M^{-1}\ s^{-1}$, suggesting that the reactions are diffusionally controlled. A biofuel cell was developed based on enzymes (producing NADH upon the biocatalytic oxidation of primary substrate) and diaphorase (electrically contacted via an electron relay and providing bioelectrocatalytic oxidation of the NADH to NAD^+, (**5**)).[60] A number of NAD^+-dependent enzymes (alcohol dehydrogenase, EC 1.1.1.1; aldehyde dehydrogenase, EC 1.2.1.5; formate dehydrogenase, EC 1.2.1.2) provided a sequence of biocatalytic reactions resulting in the oxidation of methanol to formaldehyde and finally CO_2 (Figure 4). The reduced co-factor (NADH) produced in all the steps was biocatalytically

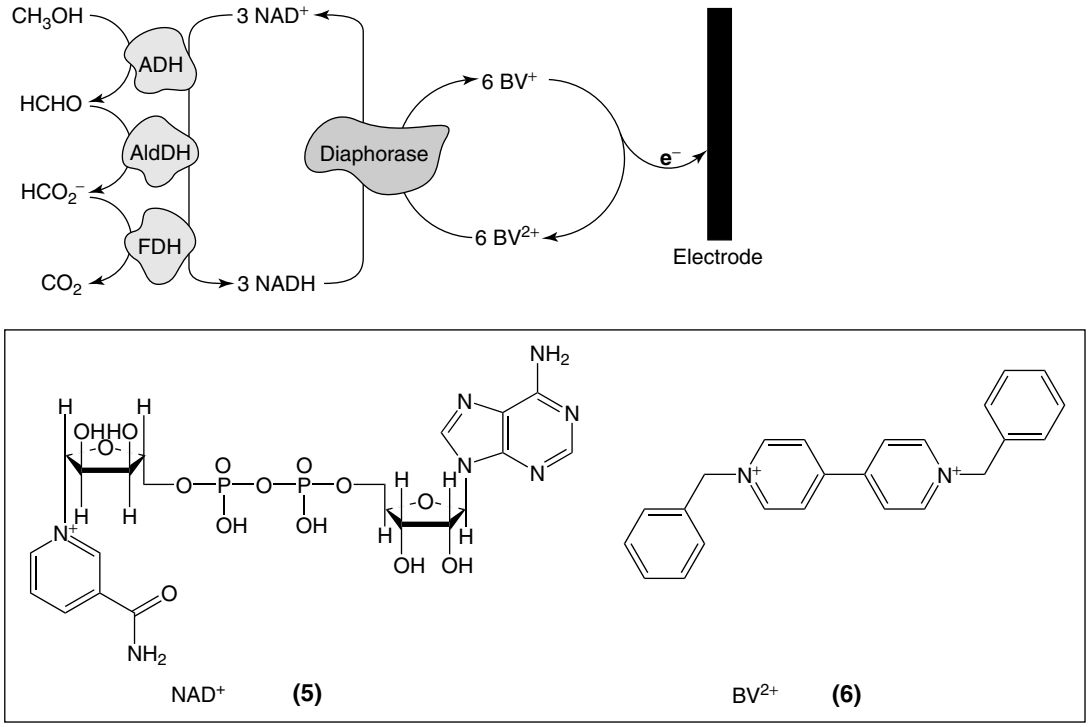

Figure 4. Schematic configuration of methanol/dioxygen biofuel cell. NAD^+-dependent dehydrogenases oxidize CH_3OH to CO_2; diaphorase (D) catalyzes the oxidation of NADH to NAD^+ using *N*,*N*′-dibenzyl-4,4-bipyridinium (benzylviologen, BV^{2+}) as the electron acceptor. BV^+ is oxidized to BV^{2+} at a graphite anode and thus, releases electrons for the reduction of dioxygen at a platinum cathode. ADH: alcohol dehydrogenase; AldDH: aldehyde dehydrogrnase; FDH: formate dehydrogenase.

oxidized by diaphorase. This diaphorase was electrochemically contacted by a diffusional electron relay (benzylviologen, BV^{2+}, (**6**)) that provided enzyme regeneration and anodic current. The biocatalytic anode was conjugated with an O_2-cathode to complete the biofuel cell. The total reaction in the biofuel cell is methanol oxidation by O_2. The biofuel cell provided $V_{oc} = 0.8\,V$ and a maximum power density of ca. $0.68\,mW\,cm^{-2}$ at 0.49 V. It should be noted, however, that this multienzyme system was utilized in a nonorganized configuration, where all biocatalysts exist as diffusional components in the cell.

In view of the high cost of $NAD(P)^+$/NAD(P)H co-factors, practical applications require their immobilization together with enzymes. Nevertheless, the covalent coupling of natural $NAD(P)^+$ co-factors to an organic support results in a substantial decrease of their functional activity. Mobility is vital for its efficient interaction with enzymes, and thus attention has been paid to the synthesis of artificial analogs of the $NAD(P)^+$ co-factors carrying functional groups separated from the bioactive site of the co-factor by spacers.[61, 62] The spacer is usually linked to *N*-6 position of the $NAD(P)^+$ molecule, and provides some flexibility for the bioactive part of the co-factors, allowing them to be associated with the enzyme molecules. Structure–activity relationships of the artificial functionalized $NAD(P)^+$-derivatives have been studied with different enzymes and the possibility to substitute natural $NAD(P)^+$ with these artificial analogs has been demonstrated.[61, 63] An efficient electrode that acts as an anode in the presence of an $NAD(P)^+$-dependent enzyme should include three integrated, electrically contacted components: The $NAD(P)^+$-co-factor that is associated with the respective enzyme and a catalyst that allows the efficient regeneration of the co-factor.

Electrodes functionalized with co-factor monolayers can form stable affinity complexes with their respective enzymes.[64–66] These interfacial complexes can be further crosslinked to produce integrated bioelectrocatalytic matrices consisting of the relay-units, the co-factor and the enzyme molecules. Electrically contacted biocatalytic electrodes of NAD^+-dependent enzymes have been organized by the generation of affinity complexes between a catalyst/NAD^+-monolayer and the respective enzymes.[65, 66] A PQQ monolayer covalently linked to an amino-functionalized NAD (N^6-(2-aminoethyl)-NAD^+, (**7**)) was assembled onto a Au-electrode (Figure 5a). The resulting monolayer-functionalized electrode binds NAD^+-dependent enzymes (e.g., L-lactate dehydrogenase

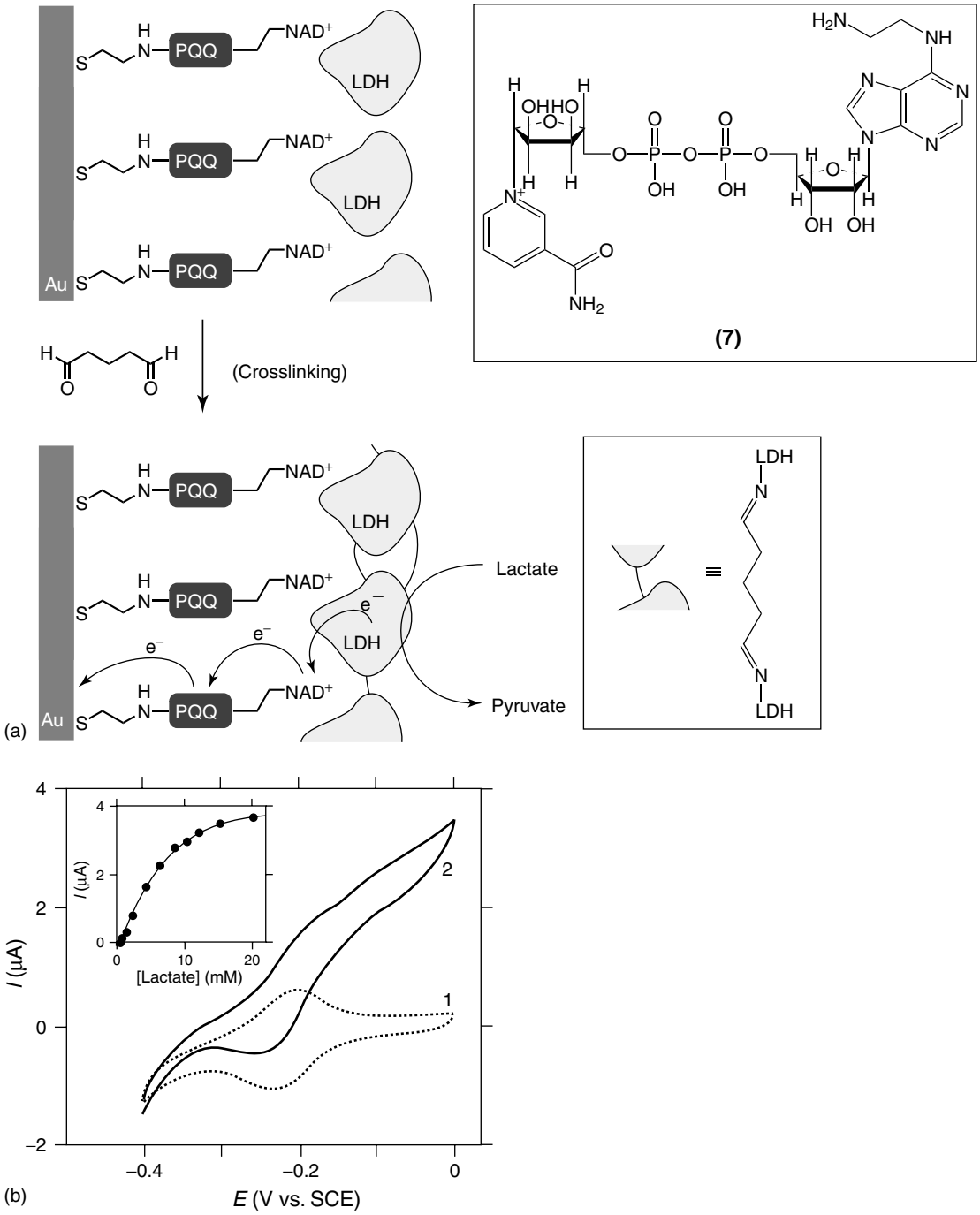

Figure 5. (a) The assembly of an integrated LDH monolayer-electrode by the crosslinking of an affinity complex formed between the LDH and a PQQ/NAD^+ monolayer-functionalized Au-electrode. (b) Cyclic voltammograms of the integrated crosslinked PQQ/NAD^+/LDH electrode (geometrical area ca. 0.2 cm^2, roughness factor ca. 15): (1) in the absence of lactate; (2) with lactate, 20 mM. Data recorded in 0.1 M Tris–buffer, pH 8.0, in the presence of 10 mM $CaCl_2$, under Ar, scan rate, 2 mV s^{-1}. Inset: Amperometric responses of the integrated electrode at different concentrations of lactate upon the application of a constant potential corresponding to 0.1 V vs. SCE. (Adopted from Scheme 4 and Figure 2 in Ref. [66]. Reprinted with permission. Copyright 1997 American Chemical Society.)

(LDH) EC 1.1.1.27) by affinity interactions between the co-factor and the biocatalyst. These enzyme electrodes electrocatalyze the oxidation of their respective substrates (e.g., lactate). The crosslinking of the enzyme layer, using glutaric dialdehyde, generates a stable, electrically contacted electrode. Figure 5(b) shows the electrical responses of a crosslinked layered PQQ/NAD^+/LDH electrode in the absence (curve 1) and the presence (curve 2) of lactate, and the inset shows the respective calibration curve corresponding to the amperometric output

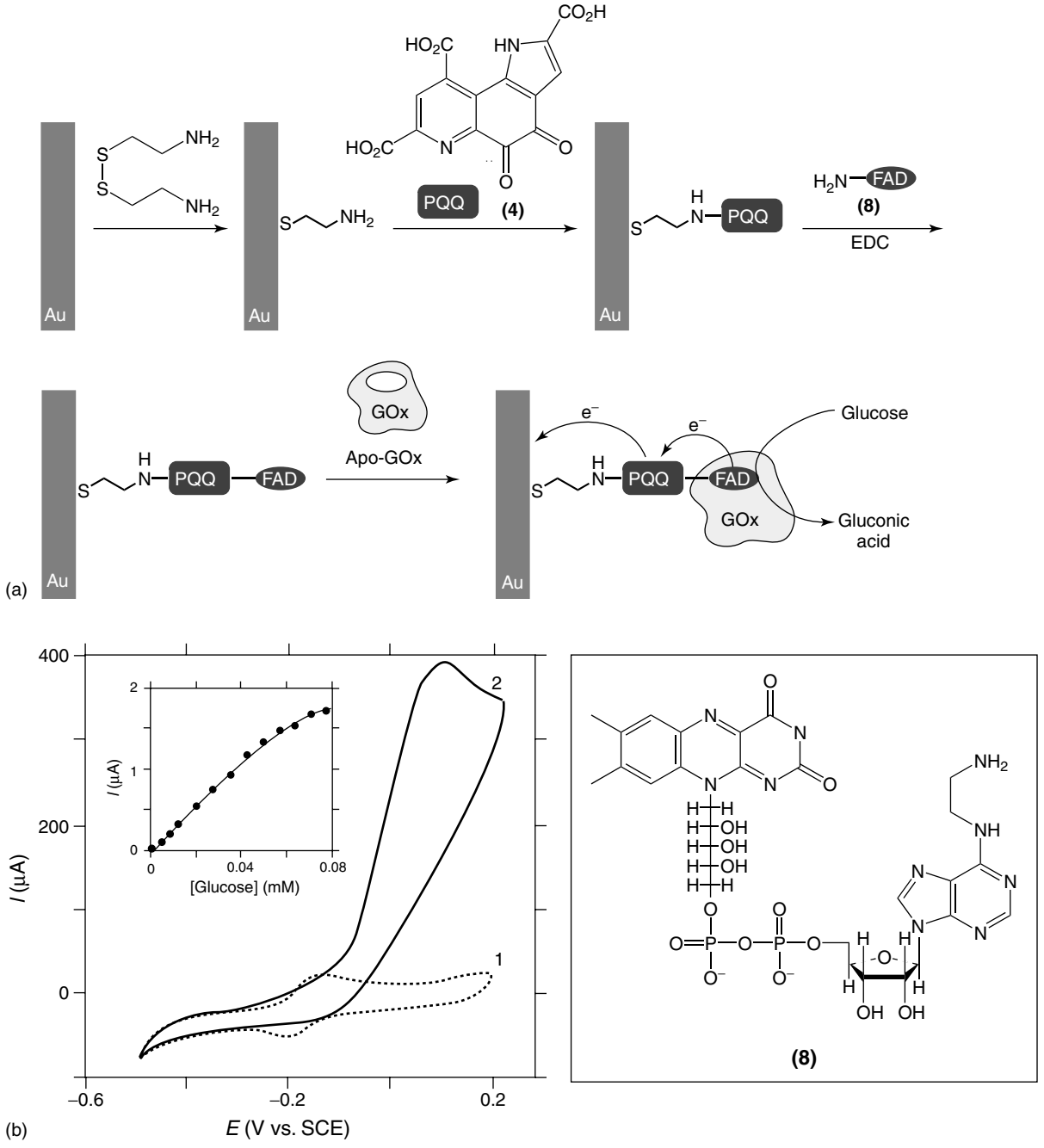

Figure 6. (a) The surface-reconstitution of apo-GOx on a PQQ-FAD monolayer assembled on a Au-electrode (geometrical area ca. 0.4 cm^2, roughness factor ca. 20). (b) Cyclic voltammograms of the GOx-reconstituted PQQ-FAD-functionalized Au-electrode: (1) in the absence of glucose; (2) with glucose, 80 mM. Recorded in 0.1 M phosphate buffer, pH 7.0, under Ar, at 35 °C, scan rate, 5 mV s^{-1}. Inset: Calibration curve corresponding to the current output (measured by chronoamperometry, $E = 0.2$ V vs. SCE) of the PQQ-FAD-reconstituted glucose oxidase enzyme-electrode at different concentrations of glucose. (Adopted from Scheme 1 and Figure 1 in Ref. [71]. Reprinted with permission. Copyright 1996 American Chemical Society.)

of the integrated LDH layered electrode at different lactate concentrations. This system exemplifies a fully integrated rigid biocatalytic matrix composed of the enzyme, co-factor and catalyst. The complex between the NAD^+-co-factor and LDH aligns the enzyme on the electrode support, thereby enabling effective electrical communication between the enzyme and the electrode, while the PQQ sites provide the regeneration of NAD^+.

3.1.2 Flavoenzyme-functionalized electrodes as anode-elements: oxidation of glucose by GOx reconstituted on an FAD/PQQ-monolayer-functionalized electrode

The electrical contacting of redox enzymes that defy direct electrical communication with electrodes can be established by using synthetic or biologically active charge carriers as intermediates between the redox center and the electrode.[10] The overall electrical efficiency of an enzyme-modified electrode depends not only on the electron transport properties of the mediator, but also on the transfer steps occurring in the assembly. Diffusional electron relays have been utilized to shuttle electrons between oxidative enzymes and anodes of biofuel cells, providing the bioelectrocatalyzed oxidation of organic fuels (e.g., methanol).[67–69] A sequence of biocatalytic reactions was applied to achieve the stepwise oxidation of methanol to CO_2. In order to accomplish superior electron contacting, the mediator may be selectively placed in an optimum position between the redox center and the enzyme periphery. In the case of surface-confined enzymes, the orientation of the enzyme-mediator assembly with respect to the electrode can also be optimized. A novel means for the establishment of electrical contact between the redox center of flavoenzymes and their environment based on a reconstitution approach has recently been demonstrated.[70]

The organization of a reconstituted enzyme aligned on an electron relay-FAD monolayer was recently realized by the reconstitution of apo-glucose oxidase (apo-GOx) on a surface functionalized with a relay-FAD monolayer (Figure 6a).[71, 72] PQQ (**4**) was covalently linked to a base cystamine monolayer at a Au-electrode, and N^6-(2-aminoethyl)-FAD (**8**) was then attached to the PQQ relay units. Apo-GOx (obtained by the extraction of the native FAD-co-factor from GOx (EC 1.1.3.4)) was then reconstituted onto the FAD units of the PQQ-FAD-monolayer architecture to yield a structurally aligned, immobilized, biocatalyst on the electrode with a surface coverage of 1.7×10^{-12} mol cm^{-2}. The resulting enzyme-reconstituted PQQ-FAD-functionalized electrode revealed bioelectrocatalytic properties. Figure 6(b) shows cyclic voltammograms of the enzyme electrode in the absence and the presence of glucose (curves a and b, respectively). When the glucose-substrate is present, an electrocatalytic anodic current is observed, implying electrical contact between the reconstituted enzyme and the electrode surface. The electrode constantly oxidizes the PQQ site located at the protein periphery, and the PQQ-mediated oxidation of the FAD-center activates the bioelectrocatalytic oxidation of glucose (equations (15)–(17)). The resulting electrical current is controlled by the recycling rate of the reduced FAD by the substrate. Figure 6(b), inset, shows the derived calibration curve corresponding to the amperometric output of the enzyme-reconstituted electrode at different concentrations of glucose. The resulting current densities are unprecedentedly high (300 mA cm^{-2} at 80 mM of glucose).

$$\mathrm{FAD} + \mathrm{glucose} + 2\mathrm{H}^+ \longrightarrow \mathrm{FADH_2} + \mathrm{gluconic\ acid} \quad (15)$$

$$\mathrm{FADH_2} + \mathrm{PQQ} \longrightarrow \mathrm{FAD} + \mathrm{PQQH_2} \quad (16)$$

$$\mathrm{PQQH_2} \longrightarrow \mathrm{PQQ} + 2\mathrm{H}^+ + 2\mathrm{e}^-(\mathrm{to\ anode}) \quad (17)$$

Control experiments reveal that without the PQQ component, the system does not exhibit electron-transfer communication with the electrode surface, demonstrating that the PQQ relay unit is, indeed, a key component in the electrooxidation of glucose.[71, 72] The electron-transfer turnover rate of GOx with molecular oxygen as the electron acceptor is around 600 s^{-1} at 25 °C. Using an activation energy of 7.2 kcal mol^{-1}, the electron-transfer turnover rate of GOx at 35 °C is estimated to be ca. 900 s^{-1}.[71, 72] A densely packed monolayer of GOx (ca. 1.7×10^{-12} mol cm^{-2}) that exhibits the theoretical electron-transfer turnover rate is expected to yield an amperometric response of ca. 300 mA cm^{-2}. This indicates that the reconstituted GOx on the PQQ-FAD monolayer exhibits an electron-transfer turnover with the electrode of similar effectiveness to that observed for the enzyme with oxygen as a natural electron acceptor. Indeed, the high current output of the resulting enzyme-electrode is preserved in the presence of O_2 in the solution.

3.2 Cathodes for biofuel cells based on enzyme-catalyzed reductive reactions

The biocatalytic reduction of oxidizers (e.g., dioxygen, hydrogen peroxide) has attracted much less attention than the biocatalytic oxidation of fuels. Nonetheless, in order to construct a biofuel cell element, it is essential to design a functional cathode for the reduction of the oxidizer that is coupled to the anode and allows the electrically balanced

current flow. Conventional O_2-reducing cathodes used in fuel cells are usually not compatible with biocatalytic anodes since high temperatures and pressures are applied for their operation. Thus, biocatalytic reductive processes at the cathode should be considered as a strategy to design all biomaterial-based functional fuel cells.

3.2.1 Bioelectrocatalytic cathodes for the reduction of peroxides

Hydrogen peroxide is a strong oxidizer ($E^{\circ\prime} = 1.535$ V vs. SCE), yet its electrochemical reduction proceeds with a very high overpotential. The bioelectrocatalyzed reduction of H_2O_2 has been accomplished in the presence of various peroxidases (e.g., horseradish peroxidase, EC 1.11.1.7).[73] Microperoxidase-11 (MP-11, (**9**)) is an oligopeptide consisting of 11 amino acids and a covalently linked Fe(III)-protoporphyrin IX heme site.[74] The oligopeptide is obtained by the controlled hydrolytic digestion of cytochrome *c* and it corresponds to the active-site microenvironment of the cytochrome. MP-11 reveals several advantages over usual peroxidases: It has a much smaller size, high stability and exhibits direct electrical communication with electrodes since its heme is exposed to the solution.

MP-11 was covalently linked to a cystamine monolayer self-assembled on a Au-electrode.[75] The MP-11 (**9**) structure suggests two different modes of coupling of the oligopeptide to the primary cystamine monolayer: (i) linkage of the carboxylic functions associated with the protoporphyrin IX ligand to the monolayer interface; (ii) coupling of carboxylic acid residues of the oligopeptide to the cystamine residues. These two modes of binding reveal similar formal potentials – $E^{\circ\prime} = -0.40$ V vs. SCE (Figure 7a). The electron transfer rates of the two binding modes of MP-11 were kinetically resolved using chronoamperometry,[76] and appear in an approximately 1 : 1 ratio. The interfacial electron transfer rates to the heme sites linked to the electrode by the two binding modes are 8.5 and 16 s^{-1}. Coulometric analysis of the MP-11 redox wave, corresponding to the reversible reduction–oxidation of the heme (equation (18)), indicates a surface coverage of 2×10^{-10} mol cm^{-2}.

$$[\text{heme–Fe(III)}] + e^- \longrightarrow [\text{heme–Fe(II)}] \qquad (18)$$

Figure 7(b) shows cyclic voltammograms of the MP-11-functionalized electrode recorded at positive potentials in the absence of H_2O_2 (curve 1) and in the presence of added H_2O_2 (curve 2). The observed electrocatalytic cathodic current indicates the effective electrobiocatalyzed reduction of H_2O_2 by the functionalized electrode. It should be noted that the electrocatalytic current for the reduction of H_2O_2 in aqueous solutions is observed at much more positive potentials than the MP-11 redox potential registered in the absence of H_2O_2 (cf. Figure 7a and b). The reason for this potential shift is the result of the formation of the Fe(IV) intermediate species in the presence of H_2O_2 (equations (19)–(21)). Control experiments reveal that no electroreduction of H_2O_2 occurs at the bare Au electrode within this potential window.

$$[\text{heme–Fe(III)}] + H_2O_2 \longrightarrow [\text{heme–Fe(IV)=O}]^{\bullet+} + H_2O \qquad (19)$$

$$[\text{heme–Fe(IV)=O}]^{\bullet+} + e^-(\text{from cathode}) + H^+ \longrightarrow [\text{heme–Fe(IV)–OH}] \qquad (20)$$

$$[\text{heme–Fe(IV)–OH}] + H^+ + e^-(\text{from cathode}) \longrightarrow [\text{heme–Fe(III)}] + H_2O \qquad (21)$$

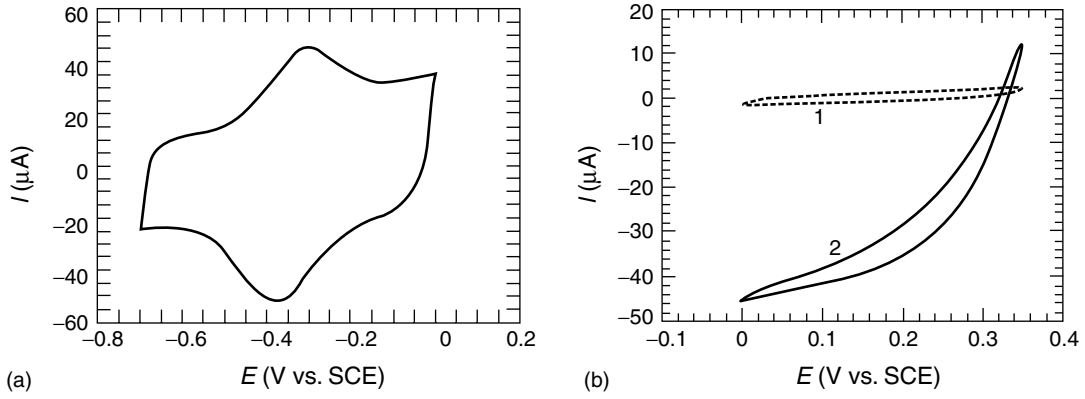

Figure 7. (a) Cyclic voltammogram of the MP-11-modified Au-electrode (geometrical area ca. 0.2 cm^2, roughness factor ca. 15) in 0.1 M phosphate buffer, pH 7.0, under Ar atmosphere, scan rate 50 mV s^{-1}. (b) Cyclic voltammograms of the MP-11 modified electrodes recorded at positive potentials in 0.1 M phosphate buffer, pH 7.0, scan rate 10 mV·s^{-1}, (1) without H_2O_2, (2) in the presence of 5 mM H_2O_2. (Adopted from Figure 3 and Figure 4 in Ref. [87]. Reproduced by permission of The Royal Society of Chemistry.)

The biocatalytic reduction of oxidizers in nonaqueous solutions immiscible with water is important since it can be coupled to biocatalytic oxidative processes through liquid/liquid interfaces. Some enzymes,[77] particularly peroxidases,[73] can function in nonaqueous solutions. A horseradish peroxidase (HRP)-modified electrode has been applied for the biocatalytic reduction of organic peroxides in nonaqueous solvents.[78] The biocatalytic activity of enzymes, particularly of HRP,[79] however, is usually lower (sometimes by an order of magnitude) in organic solvents than in water. MP-11 monolayer-modified electrodes have demonstrated high activity and stability for the electrocatalytic reduction of organic hydroperoxides in acetonitrile and ethanol.[80]

In order to perform a biocatalytic cathodic reaction in a medium immiscible with an aqueous solution, an MP-11-modified electrode was studied in a dichloromethane electrolyte (Figure 8, inset).[81] A quasi-reversible redox wave was observed for the heme center of MP-11 at $E^{\circ\prime} = -0.30\,\text{V}$ (vs. aqueous SCE, in dichloromethane that includes tetrafluoroborate). Coulometric assay of the redox wave indicated a surface coverage of ca. $3 \times 10^{-10}\,\text{mol cm}^{-2}$. Figure 8 shows cyclic voltammograms of the MP-11-functionalized electrode in the absence of an organic peroxide (curve 1), and in the presence of cumene peroxide (**10**) (curve 2). The observed electrocatalytic cathodic current indicates the effective bioelectrocatalyzed reduction of (**10**) by the functionalized electrode. The sequence of electron transfers leading to the reduction of the peroxide is summarized in equations (12) and (13). It should be noted that the MP-11 bioelectrocatalyzed reduction of organic peroxides in nonaqueous solutions does not include the intermediate formation of the Fe(IV) species, and proceeds at the MP-11 potential corresponding to the Fe(III)–Fe(II) redox transformation (equation (18)).

$$\text{[heme–Fe(II)]} + \text{Cumene peroxide (10)} \longrightarrow \text{[heme–Fe(III)]} + \text{Cumene alcohol (11)} \quad (22)$$

$$\text{[heme–Fe(III)]} + e^{-}\text{(from cathode)} \longrightarrow \text{[heme–Fe(II)]} \quad (23)$$

3.2.2 *Bioelectrocatalytic cathodes for the reduction of dioxygen*

The direct electrochemical reduction of dioxygen proceeds with very large overpotentials (e.g., at ca. −0.3 V vs. SCE at a bare Au electrode, pH 7). Thus, catalysts are required in order to utilize oxygen reduction in fuel cells. The four-electron transfer reduction of O_2 to water, without the

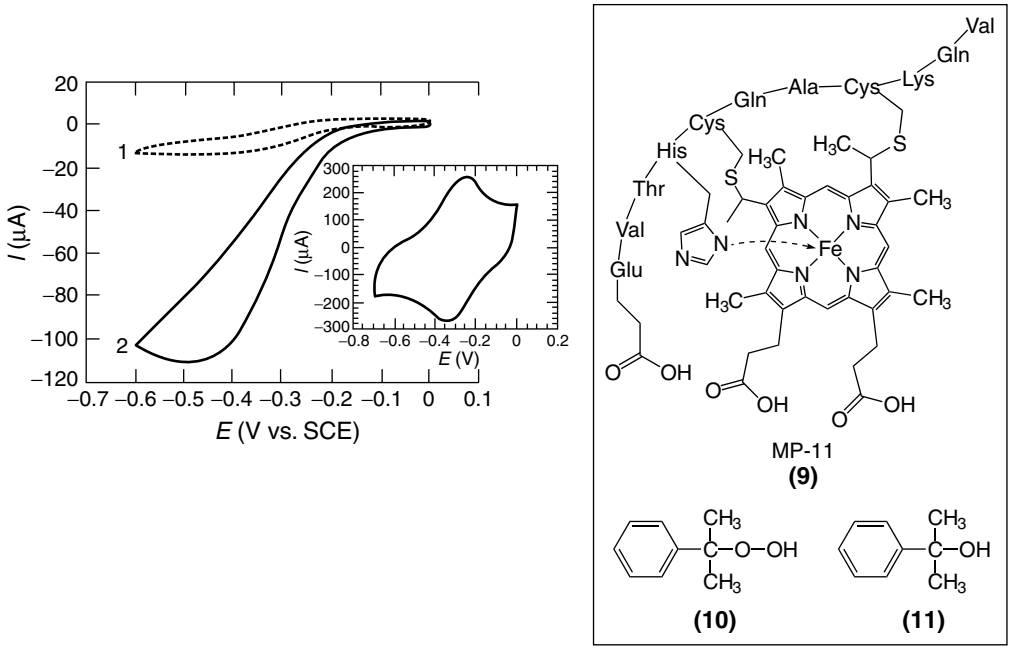

Figure 8. Cyclic voltammograms of the MP-11-functionalized Au-electrode (geometrical area ca. $0.4\,\text{cm}^2$, roughness factor ca. 20): (a) in the absence of an organic peroxide; (b) in the presence of cumene peroxide, $5 \times 10^{-3}\,\text{M}$. Potential scan rate, $5\,\text{mV s}^{-1}$. Inset: Cyclic voltammogram of the MP-11-monolayer-modified Au electrode in the absence of cumene peroxide. Potential scan rate, $50\,\text{mV s}^{-1}$; Ar atmosphere; electrolyte composed of a dichloromethane solution with 0.05 M tetra *n*-butylammonium tetraphenylborate (TBATFB). Structures of MP-11 (9), cumene peroxide (10) and cumene alcohol (11) are shown. (Adopted from Figure 1(B) in Ref. [81]. Reproduced by permission of The Royal Society of Chemistry.)

formation of peroxide or superoxide, is a major challenge for the future development of biofuel cell elements, since such reactive intermediates would degrade the biocatalysts in the system.

Biocatalytic systems composed of enzymes and their respective electron transfer mediators (e.g., bilirubin oxidase, EC 1.3.3.5,[82] or fungal laccase, EC 1.10.3.2,[83] with 2,2′-azino-bis-(3-ethylbenzothiazoline-6-sulfonate) as a mediator) are able to biocatalyze the electroreduction of O_2 to H_2O effectively at ca. 0.4 V (vs. SCE), significantly decreasing the overpotential. These systems, however, are composed of dissolved enzymes and mediators operating via a diffusional path that is unacceptable for technological applications. Organized layered enzyme systems are much more promising for their use in biocatalytic cathodes. Cytochrome *c* that includes a single thiol group at the 102-cysteine-residue (yeast iso-2-cytochrome *c* from *Saccharomyces cerevisiae*) was assembled as a monolayer on a Au-electrode by the covalent linkage of the thiol functionality to a maleimide monolayer-modified electrode as outlined in Figure 9. The quasi-reversible cyclic voltammogram of the electrode ($E^{\circ\prime} = 0.03$ V vs. SCE) (Figure 10a) indicated that the resulting heme–protein exhibits direct electrical contact with the electrode, probably the result of the structural alignment of the heme–protein on the electrode. Coulometric assay of the redox wave indicated a protein coverage of 8×10^{-12} mol cm^{-2}. Taking into account the cytochrome *c* (Cyt *c*) diameter (ca. 4.5 nm), this surface coverage corresponds to a densely packed monolayer. In a variety of biological transformations, Cyt *c* acts as

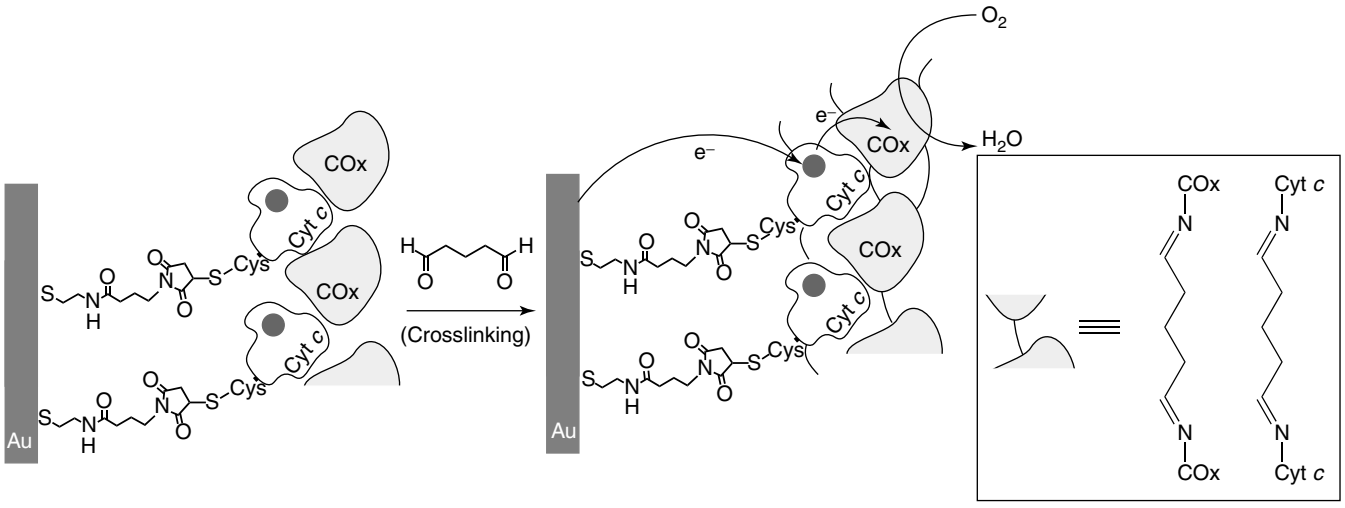

Figure 9. Assembly of the integrated bioelectrocatalytic Cyt c/COx-electrode. (Adopted from Scheme 4, ref. [85]. Reproduced by permission of The Royal Society of Chemistry.)

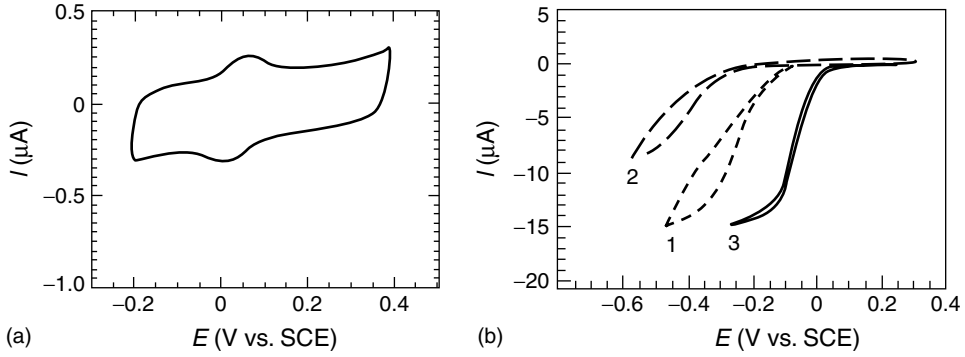

Figure 10. (a) Cyclic voltammogram of the Cyt c monolayer-modified Au-electrode (geometrical area ca. 0.2 cm^2, roughness factor ca. 1.5) measured under argon, potential scan rate 100 mV s^{-1}. (b) Cyclic voltammograms obtained in an O_2 -saturated electrolyte solution at: (1) a bare Au-electrode; (2) the Cyt c monolayer-modified Au-electrode (3) the Cyt c/Cox assembly modified Au-electrode; potential scan rate 10 mV s^{-1}. The experiments were performed in 0.1 M phosphate buffer, pH 7.0. (Adopted from Figure 1(A) and Figure 5 in Ref. [85]. Reproduced by permission of The Royal Society of Chemistry.)

an electron relay through the formation of an inter-protein complex. The association constant between the Cyt *c* monolayer and cytochrome oxidase (COx) was determined[64] to be $K_a = 1.2 \times 10^7\,M^{-1}$, and an integrated Cyt *c*/COx layered electrode was prepared as outlined in Figure 9.[84, 85] The Cyt *c* monolayer electrode was interacted with COx to generate the affinity complex on the surface, which was then crosslinked with glutaric dialdehyde. A similar Cyt *c*/COx assembly was organized on a Au-quartz crystal microbalance surface. Microgravimetric analyses indicates that the surface coverage of COx on the base Cyt *c* monolayer is ca. $2 \times 10^{-12}\,mol\,cm^{-2}$. This surface density corresponds to an almost densely packed monolayer of COx.

Figure 10(b), curve 1, shows the cyclic voltammogram of a bare Au-electrode in the presence of O_2 (the background electrolyte equilibrated with air). The cathodic wave of the O_2-electroreduction is observed at ca. −0.3 V vs. SCE. This reduction wave is negatively shifted in the presence of the Cyt *c* monolayer electrode (Figure 10b, curve 2), implying that the heme/protein layer is inactive as a biocatalyst for the reduction of O_2. In fact, the Cyt *c* monolayer enhances the overpotential for the reduction of dioxygen due to hydrophobic blocking of the electrode surface. Figure 10(b), curve 3, shows a cyclic voltammogram of the layered Cyt *c*/COx crosslinked electrode in the presence of O_2. An electrocatalytic wave is observed at ca. −0.07 V (vs. SCE), indicating that the Cyt *c*/COx layer does act as a biocatalytic interface for the reduction of dioxygen. In a control experiment, a COx monolayer was assembled on the Au-electrode without the base Cyt *c* layer. No bioelectrocatalytic activity towards the reduction of O_2 was observed. Thus, the effective bioelectrocatalyzed reduction of O_2 by the Cyt *c*/COx interface originates from the direct electrical communication between the Cyt *c* and the electrode and the electrical contact in the crosslinked Cyt *c*/COx assembly. The electron transfer to Cyt *c* is followed by electron transfer to COx, which acts as an electron storage biocatalyst for the concerted four-electron reduction of O_2, (equations (24)–(26)) (the two-electron reduction of O_2 yields H_2O_2, while a concerted four-electron reduction of O_2 generates H_2O).

$$\text{Cyt } c_{ox} + e^-(\text{from cathode}) \longrightarrow \text{Cyt } c_{red} \quad (24)$$

$$4\text{Cyt } c_{red} + \text{COx}_{ox} \longrightarrow 4\text{Cyt } c_{ox} + \text{COx}_{red} \quad (25)$$

$$\text{COx}_{red} + O_2 + 4H^+ \longrightarrow \text{COx}_{ox} + 2H_2O \quad (26)$$

Rotating disk electrode (RDE) experiments were performed to estimate the electron transfer rate constant for the overall bioelectrocatalytic process corresponding to the reduction of O_2.[85] The calculated number of electrons involved in the reduction of O_2 ($n = 3.9 \pm 0.2$) and the electrochemical rate constant ($k_{el} = 5.3 \times 10^{-4}\,cm\,s^{-1}$) were found from the Koutecky–Levich plot. The overall electron transfer rate constant ($k_{overall} = k_{el}/\Gamma_{COx} = 6.6 \times 10^5\,M^{-1}\,s^{-1}$) was calculated taking into account the surface density of the bio-electrocatalyst ($\Gamma_{COx} = 2 \times 10^{-12}\,mol\,cm^{-2}$). To determine the limiting step in the bioelectrocatalytic current formation, the experimental diffusion-limited current density ($11.6\,\mu A\,cm^{-2}$) was compared to the calculated current density assuming primary electron transfer to Cyt *c* to be the rate-limiting step. Taking into account the electron transfer rate constant to Cyt *c* ($20\,s^{-1}$) and the surface density of Cyt *c* ($\Gamma_{Cyt\,c} = 8 \times 10^{-12}\,mol\,cm^{-2}$), the calculated current density of the system is $15.5\,\mu A\,cm^{-2}$. Since the calculated current density is only slightly higher than the experimental value, it was assumed that the primary electron transfer process from the electrode to the Cyt *c* monolayer is the limiting step in the overall bioelectrocatalytic reduction of O_2. The detailed analysis of the interfacial electron-transfer rate-constants, and the use of the various electrochemical techniques to identify the kinetic parameters of the bioelectrocatalytic transformations occurring at the electrode, are described here in order to emphasize that the physical characterization of the systems is essential to optimize the electrode performance. That is, for each of the functional electrodes the complex sequence of reactions must be resolved kinetically in order to determine the rate-limiting step. Once the rate-limiting step is identified, biomaterial engineering on the respective redox protein may be undertaken in order to optimize its electron-transfer functionality, e.g., electrical communication with the electrode, inter-protein electron transfer, mediated electron transfer, etc.

3.3 Biofuel cells based on layered enzyme-electrodes

The previous sections have addressed the engineering of electrodes and the assembly of separate biocatalytic anodes and cathodes. For the design of complete biofuel cells, it is essential to couple the cathode and anode units into integrated devices. The integration of the units is not free of limitations. The oxidizer must not react with the biocatalyst relay, nor co-factor units at the anode interface, as this would decrease or prohibit the biocatalyzed oxidation of the fuel substrate. Furthermore, for synchronous operation of the biofuel cell, charge compensation between the two electrodes must be attained, and the flow of electrons in the external circuit must be compensated by cation-transport in the electrolyte solution. To overcome these limitations, the catholyte and anolyte solutions may be compartmentalized.

Alternatively, the bioelectrocatalytic transformations at the electrodes may be driven efficiently enough that interfering components do not perturb the cell operation. In any biofuel cell, either the bioelectrocatalytic transformations or the transport process is a rate-limiting step controlling the cell efficiency. The mechanistic characterization and understanding of the biofuel cell performance is therefore important as it provides a means for the further optimization of the cell efficiency.

3.3.1 A biofuel cell based on PQQ and MP-11 monolayer-functionalized electrodes

The bioelectrocatalyzed reduction of H_2O_2 by MP-11 and oxidation of NADH by PQQ has been used to design a biofuel cell using H_2O_2 and NADH as the cathodic and anodic substrates (Figure 11).[86] For the optimization of the biofuel cell element, the potentials of the functionalized electrodes were determined (vs. the reference

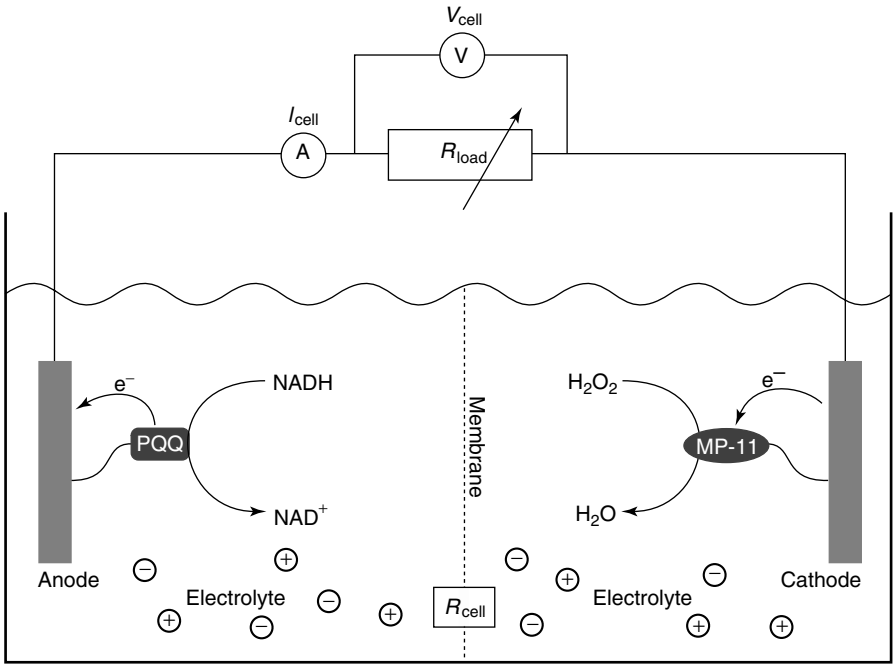

Figure 11. Schematic configuration of a biofuel cell employing NADH and H_2O_2 as fuel and oxidizer substrates and PQQ- and MP-11-functionalized-electrodes as catalytic anode and cathode, respectively. (Adopted from Scheme 1, ref. [86]. Reproduced by permission of Elsevier Science.)

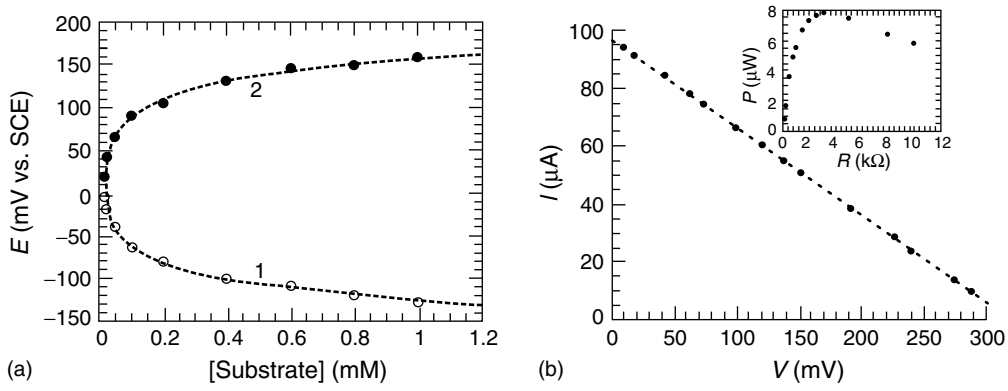

Figure 12. (a) Potentials of: (1) the PQQ-functionalized Au-electrode as a function of NADH concentration; (2) the MP-11-functionalized Au-electrode as a function of H_2O_2 concentration. The potentials of the modified electrodes were measured vs. SCE. (b) Current–voltage behavior of the PQQ-anode/MP-11-cathode biofuel cell measured at different loading resistances. Inset: electrical power extracted from the biofuel cell at different external loads. (Adopted from Figure 3 and Figure 5 in Ref. [86]. Reproduced by permission of Elsevier Science.)

electrode, SCE) as a function of the cathodic and anodic substrate concentrations. Figure 12(a) shows the potential of the PQQ-electrode at different concentrations of NADH (curve 1) and the potential of the MP-11-electrode at different H_2O_2 concentrations (curve 2). The potentials of the PQQ monolayer-electrode and the MP-11-functionalized electrode are negatively shifted and positively shifted as the concentrations of NADH and H_2O_2 are elevated, respectively. The potentials of the electrodes reveal Nernstian-type behavior reaching saturation at high substrate concentrations (ca. 1×10^{-3} M). From the saturation potential values of the PQQ- and MP-11-functionalized electrodes, an open-circuit voltage of the cell of ca. 0.3 V was estimated. Taking into account the surface density of the catalysts (1.2×10^{-10} and 2×10^{-10} mol cm^{-2} for PQQ and MP-11, respectively), their interfacial electron transfer rate constants (ca. 8 and 14 s^{-1} for PQQ and MP-11, respectively) and the number of electrons participating in a single electron transfer event (2 and 1 for PQQ and MP-11, respectively), one may derive the theoretical limit of the current densities that can be extracted by the catalytically active electrodes (ca. 185 and 270 μA cm^{-2} for the PQQ and MP-11 electrodes, respectively).

The biofuel cell performance was examined at 1×10^{-3} M of each of the fuel and oxidizer. The cell voltage rose upon increasing the external load resistance and levels off to a constant value of ca. 310 mV at ca. 50 kΩ. Upon an increase of the load resistance, the cell current dropped and reached almost zero at a resistance of ca. 50 kΩ. Figure 12(b) shows the current–voltage behavior of the biofuel cell at different external loads. The cell yields a short-circuit current (I_{sc}) and open-circuit voltage (V_{oc}) of ca. 100 μA and 310 mV, respectively. The short-circuit current density was ca. 30 μA cm^{-2}, which is almost one order of magnitude less than the theoretical limits for the catalyst-modified electrodes. Thus, the interfacial kinetics of the biocatalyzed transformations at the electrodes is probably not the current-limiting step. The power extracted from the biofuel cell ($P_{cell} = V_{cell} I_{cell}$) is shown in Figure 12(b), inset, for different external loads, and reaches a maximum of 8 μW at an external load of 3 kΩ. The ideal voltage–current relationship for an electrochemical generator of electricity is rectangular. The linear dependence observed for this biofuel cell has a significant deviation from the ideal behavior and yields a fill factor of the biofuel cell of $f \approx 0.25$ (equation (27)). This deviation from the ideal rectangular V_{cell}–I_{cell} relationship results from mass transport losses reducing the cell voltage below its reversible thermodynamic value. It should also be noted that in this study NADH is used as the fuel. In a real biofuel cell, NADH should be generated in situ from an abundant substrate and the corresponding NAD^+-dependent dehydrogenase (e.g., alcohol or lactate acid in the presence of alcohol dehydrogenase or LDH, respectively).

$$f = P_{cell} \times I_{sc}^{-1} \times V_{oc}^{-1} \tag{27}$$

3.3.2 *Biofuel cells based on GOx and MP-11 monolayer-functionalized electrodes*

The bioelectrocatalyzed reduction of H_2O_2 by the MP-11 monolayer electrode, and the oxidation of glucose by the reconstituted GOx-monolayer electrode allow us to design biofuel cells using H_2O_2 and glucose as the cathodic and anodic substrates (Figure 13).[87] Figure 14(a) shows the potentials of the GOx monolayer electrode at different concentrations of glucose (curve 1) and the potentials of the MP-11 monolayer electrode at different concentrations of H_2O_2 (curve 2). The potentials of the GOx monolayer electrode and of the MP-11 monolayer electrode are negatively shifted and positively shifted as the concentrations of the glucose and H_2O_2 are elevated, respectively. The potentials of the electrodes reveal Nernstian-type behavior, reaching saturation at high substrate concentrations of ca. 1×10^{-3} M. From the saturated potential values of the GOx and MP-11 monolayer electrodes, the theoretical limit of the open-circuit voltage of the cell is estimated to be ca. 320 mV. The short-circuit current (I_{sc}) generated by the cell is 340 μA. Taking into account the geometrical electrode area (0.2 cm^2) and the electrode roughness factor (ca. 15), the current generated by the cell can be translated into a current density of ca. 114 μA cm^{-2}. The theoretical limit of the current density extractable from the MP-11 monolayer electrode is ca. 270 μA cm^{-2} (surface coverage × interfacial electron transfer rate × Faraday constant). For the GOx monolayer electrode the maximum extractable current density was estimated to be ca. 200 μA cm^{-2} based on the surface coverage of the reconstituted GOx (1.7×10^{-12} mol cm^{-2}) and the turnover rate of the enzyme (ca. 600 s^{-1}). Thus, the observed short-circuit current density of the cell is probably controlled and limited by the bioelectrocatalyzed oxidation of glucose. This suggests that increasing the GOx content associated with the electrode could enhance the current density and the extractable power from the cell.

The biofuel cell performance was examined at concentrations of 1×10^{-3} M of each substrate. The cell voltage increases as the external load resistance is elevated, and at an external load of ca. 50 kΩ, it levels off to a constant value of ca. 310 mV. Upon increasing the external load, the current drops and is almost zero at an external load of 100 kΩ. Figure 14(b) shows the current–voltage behavior of the biofuel cell at different external loads. The linear dependence observed for the biofuel cell has

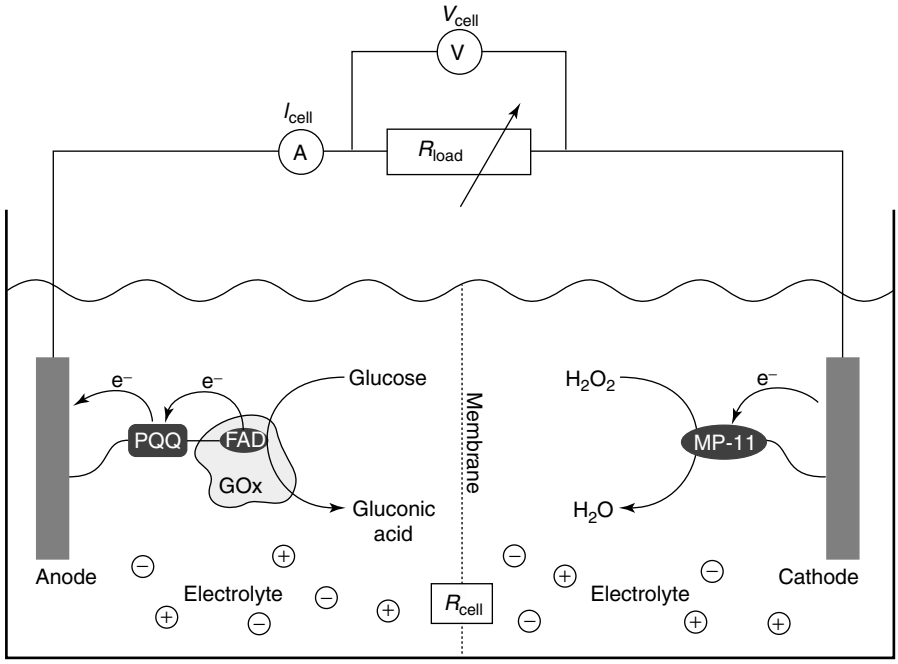

Figure 13. Schematic configuration of a biofuel cell employing glucose and H_2O_2 as a fuel and an oxidizer, respectively. GOx reconstituted onto a PQQ-FAD-monolayer and MP-11-functionalized Au-electrodes act as the biocatalytic anode and cathode, respectively. (Adopted from Scheme 3, ref. [87]. Reproduced by permission of The Royal Society of Chemistry.)

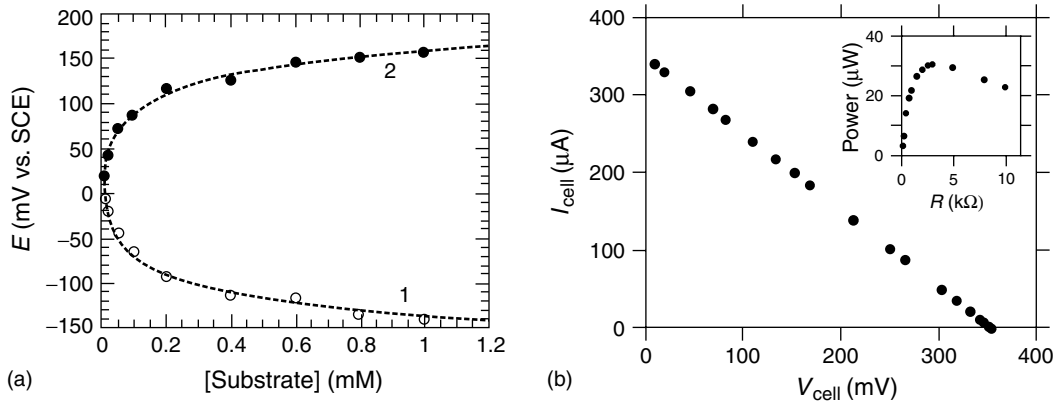

Figure 14. (a) Potential of the PQQ-FAD/GOx-modified Au-electrode as a function of glucose concentrations (1) and potential of the MP-11-functionalized Au-electrode as a function of H_2O_2 concentrations (2), potentials were measured vs. SCE. (b) Current–voltage behavior of the GOx-anode/MP-11-cathode biofuel cell at different external loads. Inset: electrical power extracted from the biofuel cell at different external loads. (Adopted from Figure 5 and Figure 7 in Ref. [87]. Reproduced by permission of The Royal Society of Chemistry.)

significant deviation from the ideal rectangular behavior and a fill factor of ca. 0.25. This deviation results from mass transport losses reducing the cell voltage below its reversible thermodynamic value. The power extracted from the biofuel element is shown in Figure 14, inset, for different external loads. The maximum power obtained is 32 μW at an external load of 3 kΩ. The biofuel cell voltage and current outputs are identical under Ar and air. This oxygen-insensitivity of the bioelectrocatalytic process at the anode originates from the effective electrical contact of the surface-reconstituted GOx with the electrode support, as a result of its alignment.[71, 72]

The stability of the biofuel cell was examined at the optimal loading resistance of 3 kΩ as a function of time.[87] The power decreases by about 50% after ca. 3 h of cell operation. This loss could originate from the depletion of

the fuel substrate, leakage of the fuel or oxidizer into the wrong compartment or the degradation of the biocatalysts. Since the cell voltage appears to be stable, the current also decreases by the same factor. Integration of the current output yields the charge that passes through the cell, and it was thus calculated that ca. 25% of the fuel was consumed upon operation of the cell for ca. 3 h. Thus, 25% of the total decrease in the current output can be attributed to the loss of the fuel concentration. Recharging the cell with the fuel substrate and oxidizer could compensate for this component of the decrease in the current output.

Charge transfer processes across the interface between two immiscible electrolyte solutions can provide an additional potential difference between cathodic and anodic reactions due to the potential difference at the liquid/liquid interface. Many different interfacial liquid/liquid systems have been studied using numerous experimental approaches.[88] The application of two immiscible solvents that exhibit perspectives for enhancing the biofuel cell output has not been used previously. The reduction of cumene peroxide in dichloromethane, electrocatalyzed by the MP-11 monolayer electrode, and the oxidation of glucose in aqueous solution, bioelectrocatalyzed by the reconstituted GOx-monolayer-electrode, enables us to design a liquid/liquid interface biofuel cell using cumene peroxide and glucose as the cathodic and anodic substrates.[81] Figure 15(a) shows the potential of the GOx-monolayer electrode at different concentrations of glucose (curve 1) and the potential of the MP-11-monolayer electrode at different concentrations of cumene peroxide in dichloromethane (curve 2). The potentials of the GOx-electrode and the MP-11-electrode are negatively and positively shifted, respectively, as the substrate concentrations are elevated. The potentials of the electrodes reveal Nernstian-type behavior, showing a logarithmic increase and reaching saturation at high concentrations of the substrates. The saturated potential values of the anode and cathode are reached at ca. 1×10^{-3} M of glucose and 1×10^{-3} M of cumene peroxide, respectively, and from the saturated potential values of the GOx- and MP-11-monolayer electrodes, the theoretical limit of the open-circuit voltage of the cell is estimated to be ca. 1.0 V. It should be noted that the potentials extrapolated to zero concentrations of the substrates show a large difference (ca. 700 mV) which results from the potential jump at the liquid/liquid interface. The phase separation of the fuel and oxidizer is the origin for the enhanced efficiency of the cell. The cell reveals an open-circuit voltage of ca. 1.0 V and a short-circuit current density of ca. 830 μA cm^{-2}. The maximum power output of the cell is 520 μW at an optimal loading resistance of 0.4 kΩ (Figure 15b).

3.3.3 *A noncompartmentalized biofuel cell based on GOx and Cyt c/Cox monolayer-electrodes*

The next generation of biofuel cells could utilize complex, ordered enzyme or multi-enzyme systems immobilized on both electrodes, that may permit the elimination of the need for compartmentalization of the anode and the cathode. The tailoring of efficient electron transfer at the enzyme-modified electrodes could enable specific biocatalytic transformations that compete kinetically with any chemical reaction of the electrode or of the biocatalysts with interfering substrates (e.g., substrate transport from

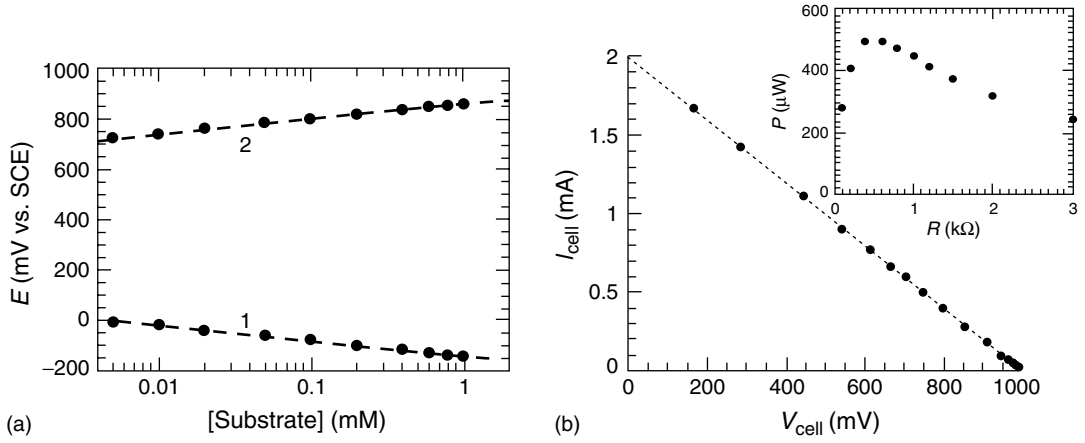

Figure 15. (a) Potential of: (1) the PQQ-AD/GOx-modified Au-electrode as a function of glucose concentration in 0.01 M phosphate buffer, pH 7.0, and 0.05 M TBATFB; (2) the MP-11-functionalized Au-electrode as a function of cumene peroxide concentration in a dichloromethane solution, 0.05 M TBATFB. Potentials were measured vs. aqueous SCE. (b) Current–voltage behavior of the biofuel cell at different external loads. Inset: electrical power extracted from the biofuel cell at different external loads. The biocatalytic cathode and anode (An discs of ca. 0.6 cm^2) were immersed in a dychloromethane solution (lower phase) and an aquous solution (upper layer), respectively. (Adopted from Figure 2 and Figure 4 in Ref. [81]. Reproduced by permission of The Royal Society of Chemistry.)

the counter compartment, oxygen, etc.). This would enable the design of noncompartmentalized biofuel cells where the biocatalytic anode and cathode are immersed in the same phase with no separating membrane. In a working example, an anode consisting of GOx reconstituted onto a PQQ-FAD monolayer (cf. Section 3.1.2) for the biocatalyzed oxidation of glucose was coupled to a cathode composed of an aligned Cyt *c*/COx couple that catalyzes the reduction of O_2 to water (cf. Section 3.2.2) (Figure 16a).[84] Since the reconstituted GOx provides extremely efficient biocatalyzed oxidation of glucose that is unaffected by oxygen, the anode can operate in the presence of oxygen. Thus, the biofuel cell uses O_2 as an oxidizer and glucose as a fuel without the need for compartmentalization. The cell operation was studied at different external loads (Figure 16b), and achieved a fill factor of ca. 40% with a maximum power output of 4 μW at an external load of 0.9 kΩ. The relatively low power extracted from the cell originates mainly from the small potential difference between the anode and cathode. The bioelectrocatalyzed oxidation of glucose occurs at the redox potential of the PQQ-electron mediator, $E^{\circ\prime} = -0.125$ V (vs. SCE at pH 7.0), whereas the redox potential of Cyt *c* is $E^{\circ\prime} = 0.03$ V. This yields a potential difference of only 155 mV

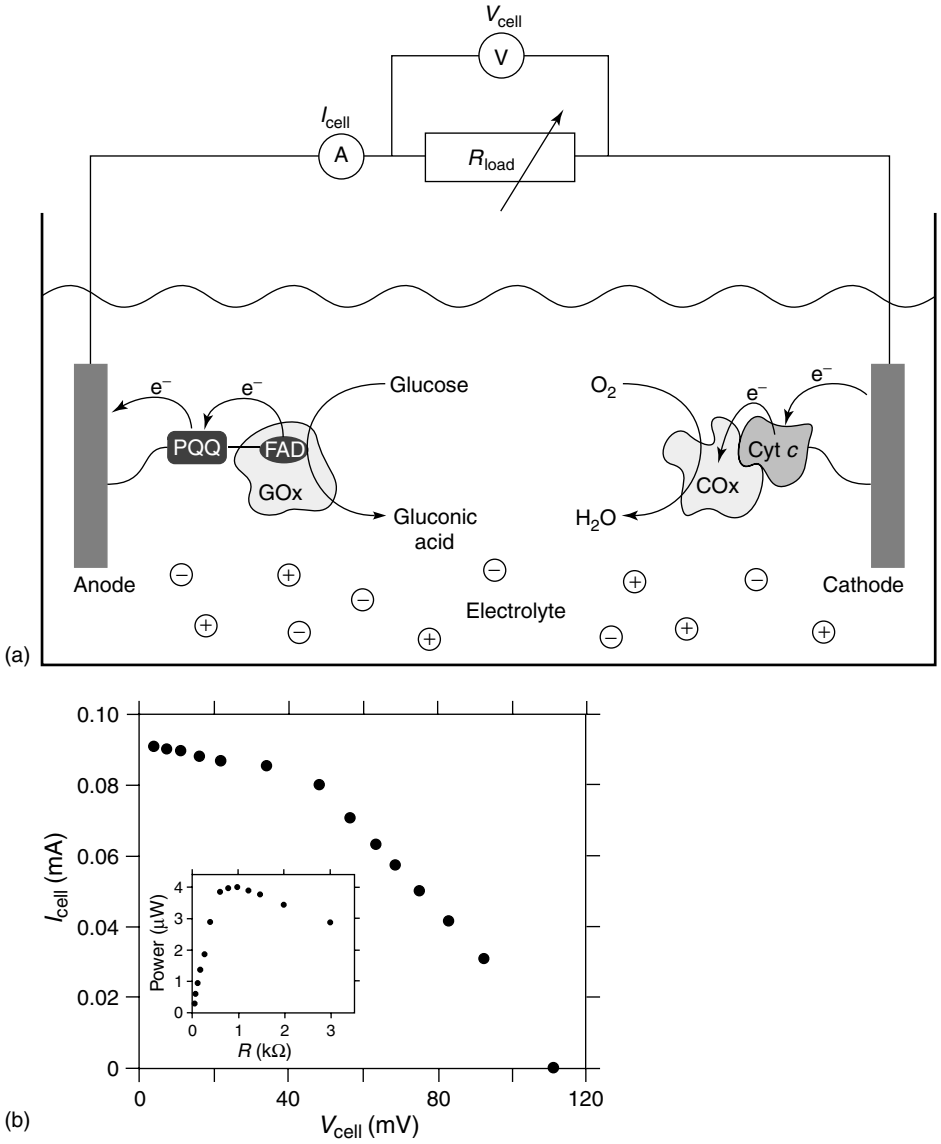

Figure 16. (a) Schematic configuration of a noncompartmentalized biofuel cell employing glucose and O_2 as fuel and oxidizer, and using PQQ-FAD/GOx and Cyt c/COx-functionalized Au-electrodes as biocatalytic anode and cathode, respectively. (b) Current–voltage behavior of the biofuel cell at different external loads. Inset: electrical power extracted from the biofuel cell at different external loads. (Adopted from Scheme 1 and Figure 1, ref. [84]. Reproduced by permission of Elsevier Science.)

between the anode and cathode. By the application of electron mediators that exhibit more negative potentials, the extractable power from the cell could be enhanced. The major advance of this system is its operation in a non-compartmentalized biofuel cell configuration. This suggests that the electrodes may be used as an in vivo electrical energy generation device utilizing as fuel and oxidizer glucose and O_2 from the bloodstream. Such in vivo electrical energy generation devices may be power sources for implantable machinery devices, e.g., pacemakers or insulin pumps.

4 CONCLUSIONS

Biofuel cells for the generation of electrical energy from abundant organic substrates can be organized by various approaches. One approach involves the use of microorganisms as biological reactors for the fermentation of raw materials to fuel products, e.g., hydrogen, that are delivered into a conventional fuel cell. The second approach to utilize microorganisms in the assembly of biofuel cells includes the in situ electrical coupling of metabolites generated in the microbial cells with the electrode support using diffusional electron mediators. A further methodology to develop biofuel cells involves the application of redox enzymes for the targeted oxidation and reduction of specific fuel and oxidizer substrates at the electrode supports and the generation of the electrical power output.

Towards this goal, it is essential to tailor integrated enzyme-electrodes that exhibit electrical contact and communication with the conductive supports. The detailed characterization of the interfacial electron transfer rates, biocatalytic rate-constants and cell resistances is essential upon the construction of the biofuel cells. Identification of the rate-limiting steps allows then the development of strategies to improve and enhance the cell output. Chemical modification of redox enzymes with synthetic units that improve the electrical contact with the electrodes provides a general means to enhance the electrical output of biofuel cells. The site-specific modification of redox enzymes and the surface-reconstitution of enzymes represent novel and attractive means to align and orient biocatalysts on electrode surfaces. The effective electrical contacting of aligned proteins with electrodes suggests that future efforts might be directed towards the development of structural mutants of redox proteins to enhance their electrical communication with electrodes. The stepwise nanoengineering of electrode surfaces with relay-co-factor-biocatalyst units by organic synthesis allows us to control the electron transfer cascades in the assemblies. By tuning the redox potentials of the synthetic relays or biocatalytic mutants, enhanced power outputs from the biofuel cells may be envisaged.

The configurations of the biofuel cells discussed in this paper can theoretically be extended to other redox enzymes and fuel substrates, allowing numerous technological applications. The production of electrical energy from biomass substrates using biofuels could complement energy sources from chemical fuel cells. An important potential use of biofuel cells is their in situ assembly in human body fluids, e.g., blood. The extractable electrical power could then be used to activate implanted devices such as pacemakers, pumps (e.g., insulin pumps), sensors and prosthetic units.

ACKNOWLEDGEMENTS

The research was supported by the Enriqus Berman Foundation.

REFERENCES

1. C. Van Dijik, C. Laane and C. Veeger, *Recl. Trav. Chim. Pays-Bas.*, **104**, 245 (1985).
2. W. J. Aston and A. P. F. Turner, *Biotechnol. Gen. Eng. Rev.*, **1**, 89 (1984).
3. L. B. Wingard Jr, C. H. Shaw and J. F. Castner, *Enzyme Microb. Technol.*, **4**, 137 (1982).
4. A. P. F. Turner, W. J. Aston, I. J. Higgins, G. Davis and H. A. O. Hill, 'Applied Aspects of Bioelectrochemistry: Fuel Cells, Sensors, and Bioorganic Synthesis', Presented at the Fourth Symposium on Biotechnology in Energy Production and Conservation, C. D. Scott (Ed), Interscience, New York, **12**, 401 (1982).
5. G. T. R. Palmore and G. M. Whitesides, 'Microbial and Enzymatic Biofuel Cells', in "Enzymatic Conversion of Biomass for Fuels Production", M. E. Himmel, J. O. Baker and R. P. Overend (Eds), ACS Symposium Series No. 566, American Chemical Society, Washington, DC, pp. 271–290 (1994).
6. A. T. Yahiro, S. M. Lee and D. O. Kimble, *Biochim. Biophys. Acta*, **88**, 375 (1964).
7. F. D. Sisler, 'Biochemical Fuel Cells', in "Progress in Industrial Microbiology", D. J. D. Hockenhull (Ed), J. & A. Churchill, London, Vol. 9, pp. 1–11 (1971).
8. S. Wilkinson, *Autonomous Robots*, **9**, 99 (2000).
9. P. N. Bartlett, P. Tebbutt and R. C. Whitaker, *Prog. Reaction Kinetics*, **16**, 55 (1991).
10. I. Willner and E. Katz, *Angew. Chem. Int. Ed.*, **39**, 1180 (2000).
11. K. Lewis, *Bacteriol. Rev.*, **30**, 101 (1966).
12. R. K. Thauer, F. H. Kirchniawy and K. A. Jungermann, *Eur. J. Biochem.*, **27**, 282 (1972).

13. S. Raeburn and J. C. Rabinowitz, *Arch. Biochem. Biophys.*, **146**, 9 (1971).
14. K. A. Jungermann, R. K. Thauer, G. Leimenstoll and K. Deker, *Biochim. Biophys. Acta*, **305**, 268 (1973).
15. R. K. Thauer, K. A. Jungermann and K. Deker, *Bacteriol. Rev.*, **41**, 100 (1977).
16. T. Akiba, H. P. Bennetto, J. L. Stirling and K. Tanaka, *Biotechnol. Lett.*, **9**, 611 (1987).
17. S. Suzuki and I. Karube, *Appl. Biochem. Bioeng.*, **4**, 281 (1983).
18. S. Suzuki, I. Karube, H. Matsuoka, S. Ueyama, H. Kawakubo, S. Isoda and T. Murahashi, *Ann. N.Y. Acad. Sci.*, **413**, 133 (1983).
19. I. Karube, S. Suzuki, T. Matunaga and S. Kuriyama, *Ann. N.Y. Acad. Sci.*, **369**, 91 (1981).
20. S. Suzuki, I. Karube, T. Matsunaga, S. Kuriyama, N. Suzuki, T. Shirogami and T. Takamura, *Biochimie*, **62**, 353 (1980).
21. I. Karube, T. Matsunaga, S. Tsuru and S. Suzuki, *Biotechnol. Bioeng.*, **19**, 1727 (1977).
22. S. Tanisho, N. Kamiya and N. Wakao, *Bioelectrochem. Bioeng.*, **21**, 25 (1989).
23. C. C. Liu, N. A. Carpenter and J. G. Schiller, *Biotechnol. Bioeng.*, **20**, 1687 (1978).
24. M. J. Cooney, E. Roschi, I. W. Marison, C. Comniellis and U. von Stockar, *Enzyme Microbiol. Technol.*, **18**, 358 (1996).
25. W. Habermann and E. H. Pommer, *Appl. Microbiol. Biotechnol.*, **35**, 128 (1991).
26. H. A. Videla and A. J. Arvia, *Biotechnol. Bioeng.*, **17**, 1529 (1975).
27. E. A. Disalvo and H. A. Videla, *Biotechnol. Bioeng.*, **23**, 1159 (1981).
28. S. J. Yao, A. J. Appleby, A. Geisel, H. R. Cash and S. K. Wolfson, Jr., *Nature*, **224**, 921 (1969).
29. S. K. Wolfson, Jr., L. B. Wingard, Jr., C. C. Liu and S. J. Yao, 'Biofuel Cells', in "Biomedical Applications of Immobilized Enzymes and Proteins", T. M. S. Chang (Ed), Plenum Press, Vol. 1, pp. 377–389 (1977).
30. M. J. Allen, 'Biofuel Cells', in "Methods in Microbiology", J. R. Norris and D. W. Ribbon (Eds), Academic Press, New York, pp. 247–283 (1972).
31. C. R. Myers and J. M. Myers, *J. Bacteriol.*, **174**, 3429 (1992).
32. H. J. Kim, M. S. Hyun, I. S. Chang and B. H. Kim, *J. Microbiol. Biotechnol.*, **9**, 365 (1999).
33. B. H. Kim, H. J. Kim, M. S. Hyun and D. H. Park, *J. Microbiol. Biotechnol.*, **9**, 127 (1999).
34. H. P. Bennetto, G. M. Delaney, J. R. Mason, S. D. Roller, J. L. Stirling and C. F. Thurston, *Biotechnol. Lett.*, **7**, 699 (1985).
35. C. F. Thurston, H. P. Bennetto, G. M. Delaney, J. R. Mason, S. D. Roller and J. L. Stirling, *J. Gen. Microbiol.*, **131**, 1393 (1985).
36. G. M. Delaney, H. P. Bennetto, J. R. Mason, S. D. Roller, J. L. Stirling and C. F. Thurston, *J. Chem. Technol. Biotechnol.*, **34B**, 13 (1984).
37. N. Kim, Y. Choi, S. Jung and S. Kim, *Biotechnol. Bioeng.*, **70**, 109 (2000).
38. S. D. Roller, H. P. Bennetto, G. M. Delaney, J. R. Mason, S. L. Stirling and C. F. Thurston, *J. Chem. Technol. Biotechnol.*, **34B**, 3 (1984).
39. H. P. Bennetto, J. L. Stirling, K. Tanaka and C. A. Vega, *Biotechnol. Bioeng.*, **25**, 559 (1983).
40. D. H. Park and J. G. Zeikus, *Appl. Environ. Microbiol.*, **66**, 1292 (2000).
41. I. Ardeleanu, D. G. Margineanu and H. Vais, *Bioelectrochem. Bioenerg.*, **11**, 273 (1983).
42. J. B. Davis and H. F. Yarbrough, Jr., *Science*, **137**, 615 (1962).
43. R. A. Patchett, A. F. Kelly and R. G. Kroll, *Appl. Microbiol. Biotechnol.*, **28**, 26 (1988).
44. G. Kreysa, D. Sell and P. Krämer, *Ber. Bunsen-ges. Phys. Chem.*, **94**, 1042 (1990).
45. C. A. Vega and I. Fernández, *Bioelectrochem. Bioeng.*, **17**, 217 (1987).
46. A. M. Lithgow, L. Romero, I. C. Sanchez, F. A. Souto and C. A. Vega, *J. Chem. Res., Synop.*, **5**, 178 (1986).
47. K. Tanaka, C. A. Vega and R. Tamamushi, *Bioelectrochem. Bioeng.*, **11**, 289 (1983).
48. D. Sell, P. Krämer and G. Kreysa, *Appl. Microbiol Biotechnol.*, **31**, 211 (1989).
49. D. H. Park, S. K. Kim, I. H. Shin and Y. J. Jeong, *Biotechnol. Lett.*, **22**, 1301 (2000).
50. R. M. Allen and H. P. Bennetto, *Appl. Biochem. Biotechnol.*, **39**, 27 (1993).
51. D. H. Park, B. H. Kim, B. Moore, H. A. O. Hill, M. K. Song and H. W. Rhee, *Biotechnol. Techniques*, **11**, 145 (1997).
52. H. A. Videla and A. J. Arvia, *Experientia*, **18**, 667 (1971).
53. W. van Hees, *J. Electrochem. Soc.*, **112**, 258 (1965).
54. M. J. Allen, *Electrochim. Acta*, **11**, 1503 (1966).
55. I. Willner and B. Willner, *Trends Biotechnol.*, **19**, 222 (2001).
56. I. Katakis and E. Dominguez, *Mikrochim. Acta*, **126**, 11 (1997).
57. B. Person, L. Gorton, G. Johansson and A. Torstensson, *Enzyme Microb. Technol.*, **7**, 549 (1985).
58. I. Willner and A. Riklin, *Anal. Chem.*, **66**, 1535 (1994).
59. E. Katz, T. Lötzbeyer, D. D. Schlereth, W. Schuhmann and H.-L. Schmidt, *J. Electroanal. Chem.*, **373**, 189 (1994).
60. G. T. R. Palmore, H. Bertschy, S. H. Bergens and G. M. Whitesides, *J. Electroanal. Chem.*, **443**, 155 (1998).
61. M. Maurice and J. Souppe, *New J. Chem.*, **14**, 301 (1990).
62. A. F. Bückmann and V. Wray, *Biotechnol. Biochem.*, **15**, 303 (1992).
63. J. Hendle, A. F. Bückmann, W. Aehle, D. Schomburg and R. D. Schmid, *Eur. J. Biochem.*, **213**, 947 (1993).
64. A. B. Kharitonov, L. Alfonta, E. Katz and I. Willner, *J. Electroanal. Chem.*, **487**, 133 (2000).
65. E. Katz, V. Heleg-Shabtai, A. Bardea, I. Willner, H. K. Rau and W. Haehnel, *Biosens. Bioelectron.*, **13**, 741 (1998).

66. A. Bardea, E. Katz, A. F. Bückmann and I. Willner, *J. Am. Chem. Soc.*, **119**, 9114 (1997).
67. E. V. Plotkin, I. J. Higgins and H. A. O. Hill, *Biotechnol. Lett.*, **3**, 187 (1981).
68. G. Davis, H. A. O. Hill, W. J. Aston, I. J. Higgins and A. P. F. Turner, *Enzyme Microb. Technol.*, **5**, 383 (1983).
69. P. L. Yue and K. Lowther, *Chem. Eng. J.*, **33**, B69 (1986).
70. A. Riklin, E. Katz, I. Willner, A. Stocker and A. F. Bückmann, *Nature*, **376**, 672 (1995).
71. I. Willner, V. Heleg-Shabtai, R. Blonder, E. Katz, G. Tao, A. F. Bückmann and A. Heller, *J. Am. Chem. Soc.*, **118**, 10 321 (1996).
72. E. Katz, A. Riklin, V. Heleg-Shabtai, I. Willner and A. F. Bückmann, *Anal. Chim. Acta*, **385**, 45 (1999).
73. T. Ruzgas, E. Csöregi, J. Emneus, L. Gorton and G. Marko-Varga, *Anal. Chim. Acta*, **330**, 123 (1996).
74. P. A. Adams, 'Microperoxidases and Iron Porphyrins', in "Peroxidases in Chemistry and Biology", J. Everse, K. E. Everse and M. B. Grisham (Eds), CRC Press, Boca Raton, FL, Vol. 2, Chapter 7, pp. 171–200 (1991).
75. T. Lötzbeyer, W. Schuhmann, E. Katz, J. Falter and H.-L. Schmidt, *J. Electroanal. Chem.*, **377**, 291 (1994).
76. E. Katz and I. Willner, *Langmuir*, **13**, 3364 (1997).
77. A. M. Klibanov, *Trends Biochem. Sci.*, **14**, 141 (1989).
78. J. Li, S. N. Tan and J. T. Oh, *J. Electroanal. Chem.*, **448**, 69 (1998).
79. L. Yang and R. W. Murray, *Anal. Chem.*, **66**, 2710 (1994).
80. A. N. J. Moore, E. Katz and I. Willner, *J. Electroanal. Chem.*, **417**, 189 (1996).
81. E. Katz, B. Filanovsky and I. Willner, *New J. Chem.*, **23**, 481 (1999).
82. S. Tsujimura, H. Tatsumi, J. Ogawa, S. Shimizu, K. Kano and T. Ikeda, *J. Electroanal. Chem.*, **496**, 69 (2001).
83. G. Tayhas, R. Palmore and H.-H. Kim, *J. Electroanal. Chem.*, **464**, 110 (1999).
84. E. Katz, I. Willner and A. B. Kotlyar, *J. Electroanal. Chem.*, **479**, 64 (1999).
85. V. Pardo-Yissar, E. Katz, I. Willner, A. B. Kotlyar, C. Sanders and H. Lill, *Faraday Discussions*, **116**, 119 (2000).
86. I. Willner, G. Arad and E. Katz, *Bioelectrochem. Bioeng.*, **44**, 209 (1998).
87. I. Willner, E. Katz, F. Patolsky and A. F. Bückmann, *J. Chem. Soc., Perkin Trans.* **2**, 1817 (1998).
88. A. G. Volkov and D. W. Deamer, 'Liquid/Liquid Interface Theory and Methods', CRC, Boca Raton, FL (1996).